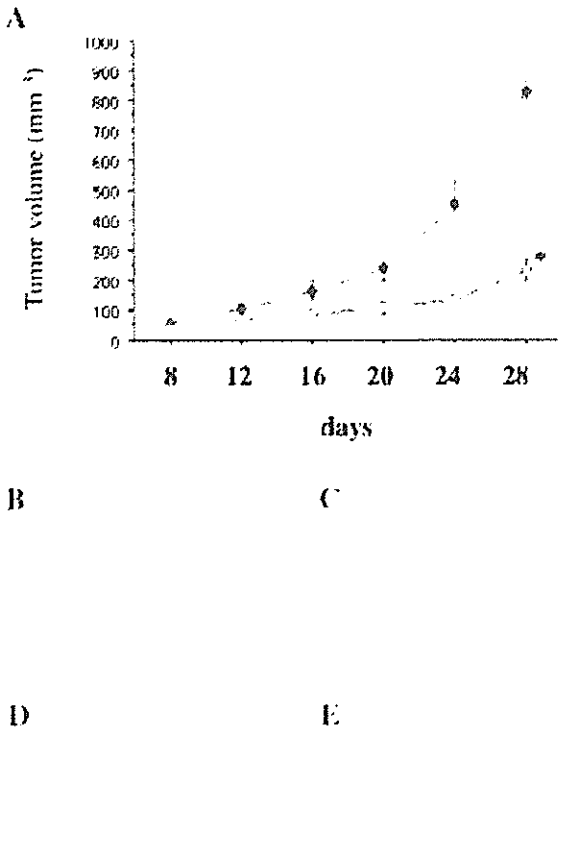

Fig. 4. A: Time course changes of tumor growth in castrated athymic nude mice by treatment with candesartan. Closed circle: control C4-2 tumor; open circle: C4-2 tumor treated with candesartan 10 mg/kg. *$P < 0.01$, compared with control C4-2 tumor. The serial photo-panels show the immunohistochemical evaluation of CD34 in the control group (B) and the treatment group (C), and that of VEGF in the control group (D) and the treatment group (E). Magnification is 1:200. The bars represent the standard error of the mean of individual experiments.

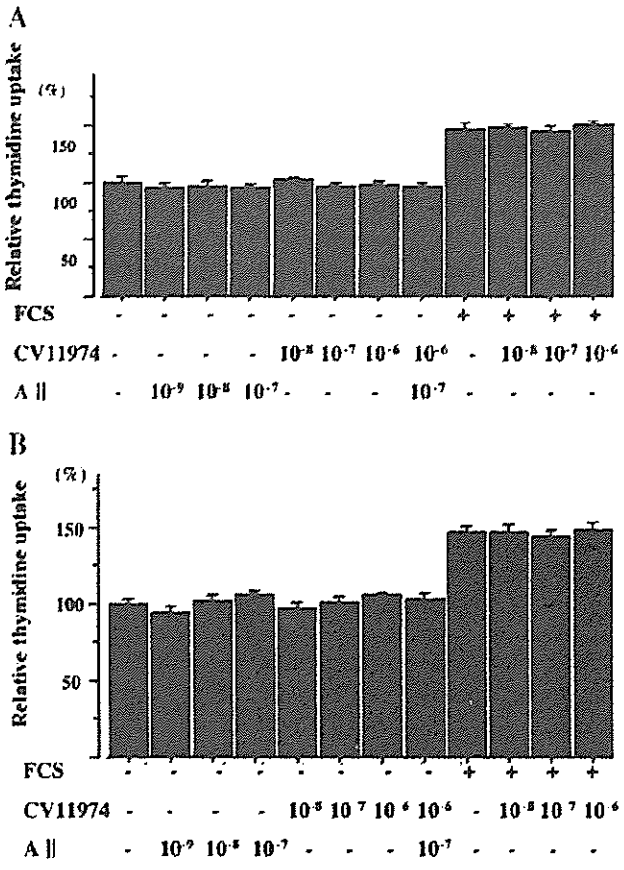

Fig. 5. Effect of AII and the ATIR antagonist (CVII974) on DNA synthesis in LNCaP cells (A) and C4-2 cells (B). The bars represent the standard error of the mean of individual experiments. FCS: 10% fetal calf serum.

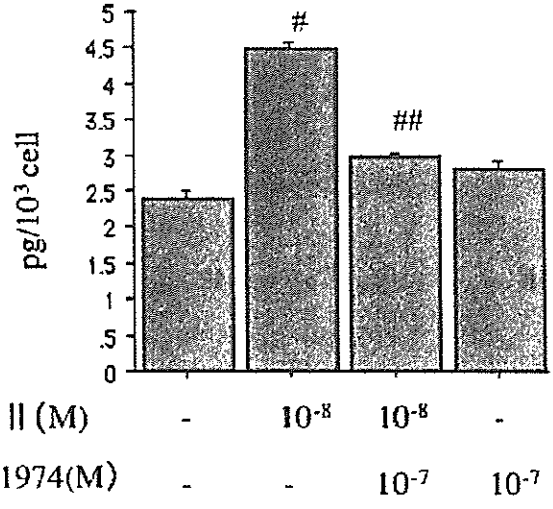

Fig. 6. VEGF measurements in C4-2 cells after 6-hr incubation. #$P < 0.01$, compared with control C4-2 cells. ##$P < 0.01$, compared to C4-2 cells treated with AII alone.

(3.0 ± 0.1 pg/10^3 cells, n = 5, $P = 0.001$). Conversely, CV11974 alone had no measurable effects on VEGF production in untreated C4-2 cells (2.8 ± 0.2 pg/10^3 cells, n = 5). Similar results were obtained with C4-2 cells at the 24-hr timepoint.

In LNCaP cells with 24-hr treatment, AII had no significant effect on VEGF synthesis (2.1 ± 0.3 pg/10^3 cells, n = 5), compared untreated LNCaP cells (2.3 ± 0.3 pg/10^3 cells, n = 5). In addition, neither CV11974 nor combination with AII and CV11974 had no significant effects on VEGF production (2.2 ± 0.2 pg/10^3 cells, n = 5; 2.1 ± 0.3 pg/10^3 cells, n = 5), compared with untreated LNCaP cells.

DISCUSSION

Recent studies have shown that MVD and VEGF expression in the primary tumor are related to the potential for recurrence and to the prognosis of patients with PCa [21,24]. Few studies have investigated angiogenesis in HRPC, although primary androgen-dependent PCa in patients without hormonal ablation has been studied several times. We evaluated AT1R expression, angiogenic factors and neovascularization in human PCa specimens obtained at surgery and autopsy. In all the samples, MVD was associated with a higher Gleason score. This finding was consistent with previous observations of prostate biopsy samples and metastatic PCa specimens [17,20,29]. Uemura et al. [30] demonstrated that AT1R expression in well-differentiated adenocarcinoma was higher than that in poorly differentiated adenocarcinoma, suggesting that AT1R expression correlated in an inverse fashion with tumor grade. Nevertheless, they recently reported that prostatic renin-angiotensin system is overexpressed in HRPC [31]. This point is, therefore, still controversial; thus we sought to determine whether HRPC overexpresses AT1R and compared AT1R expression level in a tumor xenograft model. Our clinical samples clearly demonstrated higher AT1R expression and more aggressive angiogenesis in HRPC than in surgical specimens, which were not treated endocrinologically. Additionally, C4-2 cells showed higher AT1R expression than LNCaP cells in vitro. We also created mouse xenograft models using LNCaP cells and C4-2 cells and examined them immunohistochemically. In the mouse xenograft models, C4-2 cells showed higher AT1R expression, higher MVD and higher VEGF than LNCaP cells. These results consistently support our present results obtained in human specimens and recent report [31].

Gustavsson et al. demonstrated that an androgen-independent subline, which they established as LNCaP-19, showed increased angiogenesis, which consistently supports our results. However, their study showed that LNCaP-19 expressed significantly lower VEGF and PSA secretion than control LNCaP although LNCaP-19 showed prominent tumor angiogenesis. In contrast, we found that in C4-2 cells VEGF expression was significantly higher than in LNCaP cells in vivo and they secreted higher levels of serum PSA. C4-2 cells were originally reported to secret PSA [32], and they seem to have different characteristics compared to LNCaP-19 cells. According to all our results, HRPC appeared to show higher angiogenesis, compared with untreated or androgen-dependent PCa.

The roles of the AII and AT1R pathways in tumor progression, especially by affecting cellular proliferation or tumor angiogenesis, are unclear. AII has been shown to stimulate proliferative and hypertrophic growth in vascular smooth muscle cells [33–35] and neonatal bladder stromal cells [36] by way of AT1R binding. Fujimoto suggested that candesartan had an anti-proliferative effect against pancreatic cancer [4], and Rivera et al. [37] reported that the AT1R antagonist losartan decreased the mitotic index and cell proliferation of glioma cells. In addition, Uemura demonstrated CV11974, the active form of the AT1R antagonist candesartan, inhibits the proliferation of LNCaP and DU145 cells in vitro. Nevertheless, their study was performed in 5 days, and difference between negative control and candesartan treatment group appears to be modest. Therefore, we tested the direct effect of CV11974 on tumor cell proliferation. Our study demonstrated that AII and CV11974 at clinically achievable concentration had no effect on PCa cell proliferation at any incubation time and any doses of CV11974 in LNCaP and C4-2 cells. We further confirmed similar anti-angiogenic effects of candesartan in a bladder cancer xenograft model, and also examined cytotoxic effects of CV11974 itself in several bladder cancer cell lines. That study also demonstrated no significant cytotoxic effects on those bladder cancer cell lines [13]. On the basis of our investigations in some PCa lines and most bladder cancer cell lines, we could not confirm that CV11974 inhibited cellular proliferation. Therefore we concluded that CV11974 itself does not affect cellular proliferation in vitro.

Because our results showed that AT1R expression was associated with tumor angiogenesis and HRPC growth, targeting angiogenesis via the AT1R may be a possible treatment for HRPC. We then tested the effects of candesartan in PCa xenograft models. In the C4-2 xenograft model, candesartan (10 mg/kg) caused a dramatic decrease in the volume of subcutaneous tumor nodules and serum PSA production. No such results were observed in the LNCaP xenograft model. Immunohistochemically, the candesartan treated group showed lower expression of MVD and VEGF. In vivo, candesartan significantly suppressed VEGF production in C4-2 cells under testosterone-starving condition, but not in LNCaP cells. Accordingly, we postulated that HRPC expressed higher level of VEGF spontaneously, induced angiogenesis, and metastasized easily, and that VEGF was enhanced through AT1R signaling in such cancer cells. These results suggest that the AT1R antagonist exerts its anti-tumor effect by inhibiting tumor angiogenesis. On the basis of our in vitro and in vivo experiments, we concluded that the anti-tumor effect of AT1R antagonists is not a result of direct toxicity or apoptotic induction, but of an anti-angiogenic effect.

Tumor growth and metastasis depend on the ability of a tumor to recruit blood vessels to obtain oxygen and

nutrients [14]. This process, known as angiogenesis, is driven by a variety of growth factors, including VEGF, bFGF, IGF, and TGF-β. An angiogenic switch occurs when the tumor and stroma produce more pro-angiogenic than anti-angiogenic factors. According to our results, HRPC appears to induce tumor growth with angiogenic potential, although many other differences between early and late state specimens may account for the difference. However, how HRPC triggers angiogenesis has until now been unknown. Our results clearly demonstrated that AT1R is associated with angiogenesis through VEGF production.

When a patient presents with HRPC, considerable time can elapse from a controllable state under androgen ablation to the onset of androgen independence. Nevertheless, we often treat patients with androgen ablation. The identification of factors that mediate androgen independence and its development may lead to the development of pharmacological agents that can be used to prevent the growth and metastasis of HRPC.

This study demonstrated that HRPC is characterized by higher levels of VEGF as well as angiogenesis, and that a specific AT1R blockade suppresses VEGF production, resulting in reduced tumor angiogenesis and slower progression of HRPC. Of particular interest are the findings that tumor angiogenesis is more aggressive in HRPC and that AT1R blockade suppresses HRPC tumor growth by inhibiting tumor angiogenesis in vivo, although AT1R blockade has no effects on tumor growth in vitro. Treatment with AT1R antagonists such as candesartan may have a significant impact as an innovative therapy for HRPC.

REFERENCES

1. Crawford ED, Eisenberger MA, McLeod DG, Spaulding JT, Benson R, Dorr FA, Blumenstein BA, Davis MA, Goodman PJ. A controlled trial of leuprolide with and without flutamide in prostatic carcinoma. N Engl J Med 1989;321(7):419–424.
2. Catalona WJ. Management of cancer of the prostate. N Engl J Med 1994;331(15):996–1004.
3. Helin K, Stoll M, Meffert S, Stroth U, Unger T. The role of angiotensin receptors in cardiovascular diseases. Ann Med 1997;29(1):23–29.
4. Fujimoto Y, Sasaki T, Tsuchida A, Chayama K. Angiotensin II type 1 receptor expression in human pancreatic cancer and growth inhibition by angiotensin II type 1 receptor antagonist. FEBS Lett 2001;495(3):197–200.
5. Miyajima A, Kosaka T, Asano T, Seta K, Kawai T, Hayakawa M. Angiotensin II type 1 antagonist prevents pulmonary metastasis of murine renal cancer by inhibiting tumor angiogenesis. Cancer Res 2002;62(15):4176–4179.
6. Achard JM, Pruna A, Fernandez LA, Hottelart C, Mazouz H, Rosa A, Andrejak M, Fournier A. Prevention of stroke and cancer: Could angiotensin II type 1 receptor antagonists do better than angiotensin II converting enzyme inhibitors? Am J Hypertens 1999;12(10 Pt 1):1050–1053.
7. Lever AF, Hole DJ, Gillis CR, McCallum IR, McInnes GT, MacKinnon PL, Meredith PA, Murray LS, Reid JL, Robertson JW. Do inhibitors of angiotensin-I-converting enzyme protect against risk of cancer? Lancet 1998;352(9123):179–184.
8. Le Noble FA, Hekking JW, Van Straaten HW, Slaaf DW, Struyker Boudier HA. Angiotensin II stimulates angiogenesis in the chorio-allantoic membrane of the chick embryo. Eur J Pharmacol 1991;195(2):305–306.
9. Le Noble FA, Schreurs NH, van Straaten HW, Slaaf DW, Smits JF, Rogg H, Struijker-Boudier HA. Evidence for a novel angiotensin II receptor involved in angiogenesis in chick embryo chorioallantoic membrane. Am J Physiol 1993;264(2 Pt 2):R460–465.
10. Takeda H, Kondo S. Differences between squamous cell carcinoma and keratoacanthoma in angiotensin type-1 receptor expression. Am J Pathol 2001;158(5):1633–1637.
11. Goldfarb DA, Diz DI, Tubbs RR, Ferrario CM, Novick AC. Angiotensin II receptor subtypes in the human renal cortex and renal cell carcinoma. J Urol 1994;151(1):208–213.
12. Inwang ER, Puddefoot JR, Brown CL, Goode AW, Marsigliante S, Ho MM, Payne JG, Vinson GP. Angiotensin II type 1 receptor expression in human breast tissues. Br J Cancer 1997;75(9):1279–1283.
13. Kosugi M, Miyajima A, Kikuchi E, Horiguchi Y, Murai M. Angiotensin II Type 1 receptor antagonist candesartan as an angiogenic inhibitor in a xenograft model of bladder cancer. Clin Cancer Res 2006;12(9):2888–2893.
14. Folkman J. Tumor angiogenesis: Therapeutic implications. N Engl J Med 1971;285(21):1182–1186.
15. Folkman J. Angiogenesis in cancer, vascular, rheumatoid and other disease. Nat Med 1995;1(1):27–31.
16. Hanahan D, Folkman J. Patterns and emerging mechanisms of the angiogenic switch during tumorigenesis. Cell 1996;86(3):353–364.
17. Weidner N, Carroll PR, Flax J, Blumenfeld W, Folkman J. Tumor angiogenesis correlates with metastasis in invasive prostate carcinoma. Am J Pathol 1993;143(2):401–409.
18. Brawer MK, Deering RE, Brown M, Preston SD, Bigler SA. Predictors of pathologic stage in prostatic carcinoma. The role of neovascularity. Cancer 1994;73(3):678–687.
19. Silberman MA, Partin AW, Veltri RW, Epstein JI. Tumor angiogenesis correlates with progression after radical prostatectomy but not with pathologic stage in Gleason sum 5 to 7 adenocarcinoma of the prostate. Cancer 1997;79(4):772–779.
20. Borre M, Offersen BV, Nerstrom B, Overgaard J. Microvessel density predicts survival in prostate cancer patients subjected to watchful waiting. Br J Cancer 1998;78(7):940–944.
21. Lissbrant IF, Stattin P, Damber JE, Bergh A. Vascular density is a predictor of cancer-specific survival in prostatic carcinoma. Prostate 1997;33(1):38–45.
22. Jackson MW, Bentel JM, Tilley WD. Vascular endothelial growth factor (VEGF) expression in prostate cancer and benign prostatic hyperplasia. J Urol 1997;157(6):2323–2328.
23. Ferrer FA, Miller LJ, Andrawis RI, Kurtzman SH, Albertsen PC, Laudone VP, Kreutzer DL. Vascular endothelial growth factor (VEGF) expression in human prostate cancer: In situ and in vitro expression of VEGF by human prostate cancer cells. J Urol 1997;157(6):2329–2333.
24. Borre M, Nerstrom B, Overgaard J. Association between immunohistochemical expression of vascular endothelial growth factor (VEGF), VEGF-expressing neuroendocrine-differentiated tumor cells, and outcome in prostate cancer patients

subjected to watchful waiting. Clin Cancer Res 2000;6(5):1882–1890.

25. Shimazaki J, Fuse H, Akimoto S, Sumiya H, Akakura K, Ichikawa T. Prostatic carcinoma. I: Androgen dependency of prostatic carcinoma. Gan To Kagaku Ryoho 1988;15(4 Pt 2-1):909–916.
26. Schroder FH. Endocrine treatment of prostate cancer—recent developments and the future. Part I: Maximal androgen blockade, early vs delayed endocrine treatment and side-effects. BJU Int 1999;83(2):161–170.
27. Gustavsson H, Welen K, Damber JE. Transition of an androgen-dependent human prostate cancer cell line into an androgen-independent subline is associated with increased angiogenesis. Prostate 2005;62(4):364–373.
28. Wu HC, Hsieh JT, Gleave ME, Brown NM, Pathak S, Chung LW. Derivation of androgen-independent human LNCaP prostatic cancer cell sublines: Role of bone stromal cells. Int J Cancer 1994;57(3):406–412.
29. Bettencourt MC, Bauer JJ, Sesterhenn IA, Connelly RR, Moul JW. CD34 immunohistochemical assessment of angiogenesis as a prognostic marker for prostate cancer recurrence after radical prostatectomy. J Urol 1998;160(2):459–465.
30. Uemura H, Hasumi H, Kawahara T, Sugiura S, Miyoshi Y, Nakaigawa N, Teranishi J, Noguchi K, Ishiguro H, Kubota Y. Pilot study of angiotensin II receptor blocker in advanced hormone-refractory prostate cancer. Int J Clin Oncol 2005; 10(6):405–410.
31. Uemura H, Hasumi H, Ishiguro H, Teranishi JI, Miyoshi Y, Kubota Y. Renin-angiotensin system is an important factor in hormone refractory prostate cancer. Prostate 2006;66:822–830.
32. Thalmann GN, Sikes RA, Chang SM, Johnston DA, von Eschenbach AC, Chung LW. Suramin-induced decrease in prostate-specific antigen expression with no effect on tumor growth in the LNCaP model of human prostate cancer. J Natl Cancer Inst 1996;88(12):794–801.
33. Gibbons GH, Pratt RE, Dzau VJ. Vascular smooth muscle cell hypertrophy vs. hyperplasia. Autocrine transforming growth factor-beta 1 expression determines growth response to angiotensin II. J Clin Invest 1992;90(2):456–461.
34. Itoh H, Mukoyama M, Pratt RE, Gibbons GH, Dzau VJ. Multiple autocrine growth factors modulate vascular smooth muscle cell growth response to angiotensin II. J Clin Invest 1993;91(5):2268–2274.
35. Naftilan AJ, Pratt RE, Dzau VJ. Induction of platelet-derived growth factor A-chain and c-myc gene expressions by angiotensin II in cultured rat vascular smooth muscle cells. J Clin Invest 1989;83(4):1419–1424.
36. Cheng FY, Grammatopoulos T, Lee C, Sensibar J, Decker R, Kaplan WE, Maizels M, Firlit CF. Angiotensin II and basic fibroblast growth factor induce neonatal bladder stromal cell mitogenesis. J Urol 1996;156(2 Pt 2):593–597.
37. Rivera E, Arrieta O, Guevara P, Duarte-Rojo A, Sotelo J. AT1 receptor is present in glioma cells; its blockage reduces the growth of rat glioma. Br J Cancer 2001;85(9):1396–1399.

Available online at www.sciencedirect.com
ScienceDirect
Biochemical and Biophysical Research Communications 349 (2006) 277–283
BBRC
www.elsevier.com/locate/ybbrc

Brain- and heart-specific *Patched-1* containing exon 12b is a dominant negative isoform and is expressed in medulloblastomas ☆

Hideki Uchikawa [a,b], Masashi Toyoda [a], Kazuaki Nagao [a], Hiroshi Miyauchi [c], Ryo Nishikawa [c], Katsunori Fujii [b], Yoichi Kohno [b], Masao Yamada [a], Toshiyuki Miyashita [a,*]

[a] *Department of Genetics, National Research Institute for Child Health and Development, Tokyo 157-8535, Japan*
[b] *Department of Pediatrics, Graduate School of Medicine, Chiba University, Chiba 260-8670, Japan*
[c] *Department of Neurosurgery, Saitama Medical School, Saitama 350-0495, Japan*

Received 31 July 2006
Available online 17 August 2006

Abstract

Mutations in the human tumor suppressor gene, *Patched-1*, are associated with nevoid basal cell carcinoma syndrome characterized by developmental abnormalities and tumorigenesis, such as basal cell carcinoma and medulloblastoma. During the investigation of complex alternative splicing in *Patched-1*, we identified an alternative exon, exon 12b, located between exon 12 and 13, both in humans and in mice. Since exon 12b has an in-frame stop codon, the mRNA isoform containing this exon (*Patched12b*) encodes a truncated patched-1 protein. RT-PCR and whole mount *in situ* hybridization revealed that mouse exon 12b was expressed in the brain and heart, particularly in the cerebellum, in both adults and embryos. We next performed a functional analysis of *Patched12b* using a GLI-responsive luciferase reporter. Luciferase activity was suppressed when transfected with a plasmid encoding *Patched-1*, but not with a plasmid for *Patched12b*. The suppressive activity of Patched-1 was relieved when cotransfected with a plasmid for *Patched12b*. This implies that the Patched12b protein has a dominant negative effect on Patched-1. Interestingly, *Patched12b* was found to be expressed in some of the medulloblastoma tissues and cell lines, indicating an important role in the pathogenesis of medulloblastoma as well as brain development.

Keywords: Alternative splicing; Medulloblastoma; Nevoid basal cell carcinoma syndrome; Patched-1

The *Patched-1* gene (*Ptc1*) controls cell growth and specification of the developing and postnatal tissues of many animals [1]. The nevoid basal cell carcinoma syndrome (NBCCS), also called Gorlin syndrome, is associated with mutations in a human *Ptc1* homolog, *PTCH* [2,3]. NBCCS is an autosomal dominant neurocutaneous disorder characterized by developmental malformations, such as syndactyly and spina bifida, and an increased incidence of a variety of tumors, including basal cell carcinoma (BCC) and medulloblastoma [4]. Mutations of *PTCH* are also detected in a small fraction of holoprosencephaly characterized by a failure of the complete separation of the forebrain into right and left halves [5]. Heterozygous loss of *PTCH* found in certain sporadic and familial cases of BCC and medulloblastoma indicates that *PTCH* is also a tumor suppressor gene [6–8]. Ptc1, a 12-pass transmembrane protein, is the ligand-binding component of the receptor complex for a secreted protein, Sonic hedgehog (Shh). In the absence of Shh binding, Ptc1 is thought to hold Smoothened (Smo), another component of the Shh receptor, in an inactive state and thus inhibit signaling to

☆ *Abbreviations:* AS, alternative splicing; BCC, basal cell carcinoma; EGFP, enhanced green fluorescent protein; NBCCS, nevoid basal cell carcinoma syndrome; NMD, nonsense-mediated mRNA decay; PTC, premature termination codon; Shh, Sonic hedgehog.

* Corresponding author. Fax: +81 3 5494 7035.
E-mail address: tmiyashita@nch.go.jp (T. Miyashita).

0006-291X/$ - see front matter © 2006 Elsevier Inc. All rights reserved.
doi:10.1016/j.bbrc.2006.08.046

downstream genes. Upon the binding of Shh, the inhibition of Smo is released and signaling is transduced, leading to the activation of target genes by the Gli family of transcription factors [1].

We and others have identified a number of *PTCH* mRNA isoforms generated by alternative splicing (AS) [9–11]. Among these isoforms, the one containing exon 12b conserved in both humans and mice (*PTCH12b* and *Ptc12b*, respectively) is particularly interesting since it is expressed in a brain- and heart-specific fashion, at least in human tissues [12]. Here, we show that mouse *Ptc12b* is also preferentially expressed in the brain and in the heart. Since this isoform has an in-frame stop codon, it encodes truncated Ptc1, which does not seem to have any functions. However, the functional analysis of this isoform demonstrated that it functions as a dominant negative isoform against Ptc1. Furthermore, *PTCH12b* was found to be expressed in some of the medulloblastoma tissues and cell lines, indicating an important role in the pathogenesis of medulloblastomas as well as brain development.

Materials and methods

Constructs. The plasmids for myc-PTCH and 8 × GLI-Luc were kindly provided by Dr. J. Ming and Dr. S. Ishii, respectively. Mouse *Ptc1* cDNA sequence, exon 12-12b-13, was amplified by RT-PCR. The primers used for the amplification were 5′-TTCTCCCTCCAGTACTGATG-3′ (exon 12 forward), 5′-CACCACAGCAGCCTTGGGAG-3′ (exon 13 reverse). The PCR product was subcloned into pGEM-T Easy (Promega) and used for *in situ* hybridization. pMyc-PTCH and pMyc-PTCH12b were described previously [12]. To produce pPTCH-EGFP and pPTCH12b-EGFP, *PTCH* sequences for exon 1a-exon23 and exon 1a-exon12b, respectively, were amplified by PCR using pMyc-PTCHM or pMyc-PTCH12b as a template and subcloned into pEGFP-N3 (Clontech). The primers used for the amplification were 5′-GGGGTACCGCTATGGGGAAGGCTA CTGG-3′ (exon 1a-2 forward), 5′-CGGGATCCGTTGGAGCTGCTT CCCCGGG-3′ (exon 23 reverse), and 5′-CGGGATCCCTCCTCG TAAGGAAACCTCATGTA-3′ (exon 12b reverse). Restriction enzyme recognition sequences (underlined) were added to facilitate subcloning.

RT-PCR. Total RNA was extracted using the RNeasy kit from Qiagen according to the manufacturer's recommendations. RT-PCR was performed as previously described using 5 μg of total RNA [11]. Primers used for RT-PCR were 5′-TGGCCCATGCATTCAGTGAAACA-3′ (mouse exon 11 forward), 5′-GAGGGTCATACTCTGTGCGGA-3′ (mouse exon 14 reverse), 5′-GTGTTGGTGTGGATGATGTTT-3′ (human exon 11 forward), and 5′-CGGGATCCTTGTAAAACAGCAGAAAAT-3′ (human exon 13 reverse).

Western blotting. Immunoblot analysis was performed as described previously [13]. In brief, 30 μg of the cell lysate was subjected to SDS–PAGE and transferred onto a nitrocellulose membrane. The membrane was incubated with anti-c-Myc mouse monoclonal antibody (Santa Cruz, 9E10) followed by horseradish peroxidase-conjugated anti-mouse immunoglobulins (DAKO) or with anti-GFP rabbit polyclonal antibody (Medical & Biological Laboratories, Japan) followed by horseradish peroxidase-conjugated anti-rabbit IgG (Santa Cruz).

Luciferase assay. I-23 cells growing on six-well plates were cotransfected using Effectene reagent (Qiagen) with various combinations of plasmids as indicated in Fig. 4. The total amount of transfected DNA was adjusted to 3 μg with an empty plasmid, pcDNA3.0. Twenty-four hours after the transfection, cells were harvested and subjected to the luciferase assay with the reagents and protocols provided by Promega. Firefly luciferase activity was normalized by Renilla luciferase activity from a cotransfected pRL-SV40 (Promega).

In situ hybridization. The plasmids described above were linearized and digoxigenin-labeled cRNA probes were synthesized using T7 or SP6 RNA polymerase. E10.5 embryos on a C57BL/6J background were fixed in 4% paraformaldehyde in PBS, dehydrated in methanol, and stored at −20 °C. For hybridization, embryos were rehydrated in 0.1% Tween 20 in PBS (PBT) and incubated with proteinase K (10 μg/ml in PBT) for 15 min at 37 °C. Digestion was stopped by washing with 2 mg/ml glycine in PBT, and embryos were refixed in 4% paraformaldehyde and 0.25% glutaraldehyde in PBT, washed in PBT, and hybridized overnight at 65 °C with 2 μg/ml of digoxigenin-labeled RNA probes in hybridization solution (50% formamide, 5 × SSC, 2% blocking powder (Roche), 0.1% Tween 20, 0.5% CHAPS, 50 μg/ml yeast RNA, 5 mM EDTA, and 50 μg/ml heparin). Embryos were washed in hybridization solution and in 2 × SSC, 0.1% CHAPS at 65 °C, and incubated for 30 min with 20 μg/ml RNase A in 2 × SSC, 0.1% CHAPS at 37 °C. After washing, embryos were blocked for 3 h in 10% sheep serum, 1% BSA in PBT and incubated overnight at 4 °C with anti-digoxigenin antibody (Roche) (1:2000 diluted in 10% sheep serum, 1% BSA in PBT with 1.5 mg/ml mouse embryo powder). Embryos were washed 5 times in 1% BSA in PBT for 1 h each, 3 times in NTMT (100 mM NaCl, 100 mM Tris–HCl, pH 9.5, 50 mM $MgCl_2$, and 0.1% Tween 20) for 10 min each, and stained with NBT/BCIP stock solution (Roche) (1:50 diluted in NTMT) for about 2 h at room temperature.

Immunostaining and confocal microscopy. Immunostaining was performed essentially as described previously [14]. Briefly, HeLa cells were seeded on chamber slides (Nalge Nunc International) and were transfected with the constructs indicated in the figure legend. After 24 h, the slides were fixed with 4% paraformaldehyde, permeabilized, stained with anti-c-myc antibody (Santa Cruz, 9E10) followed with FITC-labeled anti-mouse immunoglobulins (DAKO), and observed with an Olympus microscope FV300. Nuclear localization was confirmed by Hoechst33342 staining. EGFP fusion proteins were observed as described previously [15].

Results

Tissue-specific regulation of Ptc12b expression in mice

Previously, we identified a *patched-1* isoform containing a novel exon, exon 12b, between exon 12 and exon 13 both in humans (*PTCH12b*) and in mice (*Ptc12b*) (GenBank Accession Nos. AB214500 and AB214501, respectively) [12]. Using RT-PCR and exon junction microarrays, *PTCH12b* was demonstrated to be expressed in a brain- and heart-specific fashion [12]. The nucleotide sequence of and adjacent to exon12b was relatively conserved in humans and in mice, especially around the 3′-end of the exon (Fig. 1A). Since premature termination codons (PTCs) were identified in both exons, they are expected to encode proteins truncated just after the sterol-sensing domain (Fig. 1B), whose function in PTCH remains elusive [16]. The splicing regulatory element, UGCAUG, reported to be phylogenetically and spatially conserved in introns that flank the brain-enriched alternative exons [17] was found in the intron regions upstream and downstream of exon 12b in both species (Fig. 1C), supporting the hypothesis that this element is a critical component for tissue-specific splicing events. We next investigated whether exon 12b was also preferentially

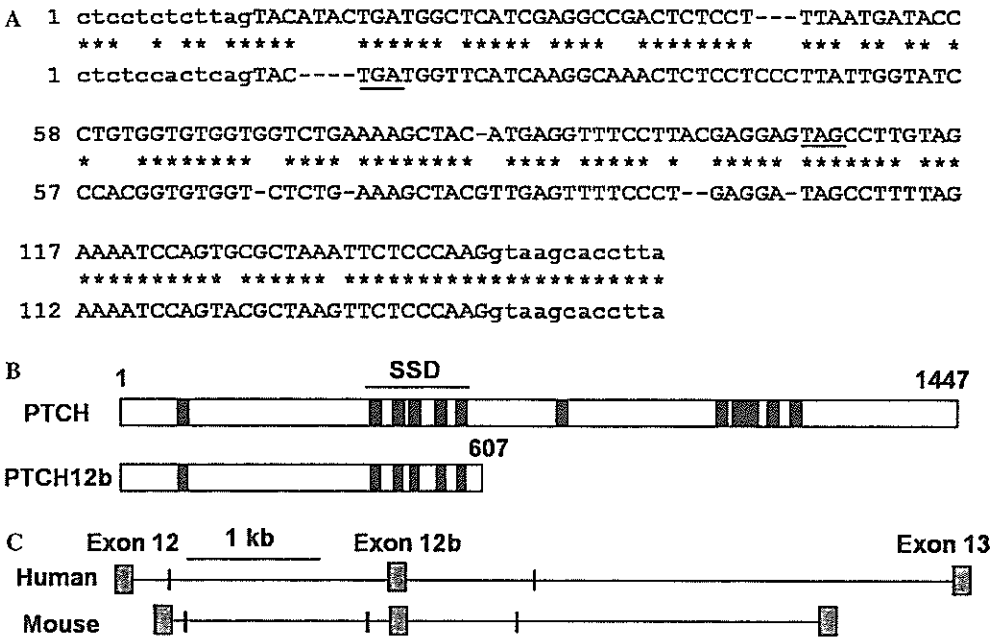

Fig. 1. Exon 12b and flanking splicing elements are conserved in humans and in mice. (A) Alignment of human (upper) and murine (lower) exon 12b and surrounding sequences. Upper- and lowercase letters indicate the exon and intron sequences, respectively. Nucleotides are numbered arbitrarily. Conserved nucleotides are marked by asterisks. In-frame stop codons are underlined. (B) PTCH protein isoforms. Numbers refer to amino acid positions relative to the first methionine of PTCH (NM_000264). Transmembrane domains are indicated by filled boxes. The region containing the 2nd to 6th transmembrane domains comprises the sterol-sensing domain (SSD). (C) Location of UGCAUG hexamers near exon 12b. The location of hexamers is indicated by small vertical thick lines.

expressed in the mouse brain and heart. In adult mice, *Ptc1* (12b−) was more or less expressed in various tissues. However, the *Ptc12b* isoform (12b+) was specifically expressed in the brain and in the heart, particularly in the cerebellum, but not in other tissues, such as the testis and the liver (Fig. 2A). To investigate the expression pattern in the mouse embryo, we performed whole mount *in situ* hybridization. *Ptc12b* was also expressed in the brain and in the heart (Fig. 2B), indicating some role yet to be identified in the development of these tissues. The specificity of the result was confirmed by the negative staining with the sense probe. Taken together, these results imply that the tissue-specific expression of this isoform is evolutionarily conserved.

PTCH12b is expressed in some medulloblastoma tissues and cell lines

Individuals with NBCCS are at high risk of medulloblastomas, which are primitive neuroectodermal tumors. Since medulloblastoma commonly arises in the cerebellum where *PTCH12b* is specifically expressed, we next addressed the question if this isoform is expressed in medulloblastoma cell lines and tissues. Out of 5 medulloblastoma cell lines analyzed, I-23 expressed very high level of *PTCH12b*. None of the 9 non-medulloblastoma cell lines expressed *PTCH12b*. Interestingly, it was also expressed in two out of two medulloblastoma tissues we examined, indicating that this isoform plays a role in the formation of medulloblastoma (Fig. 3A).

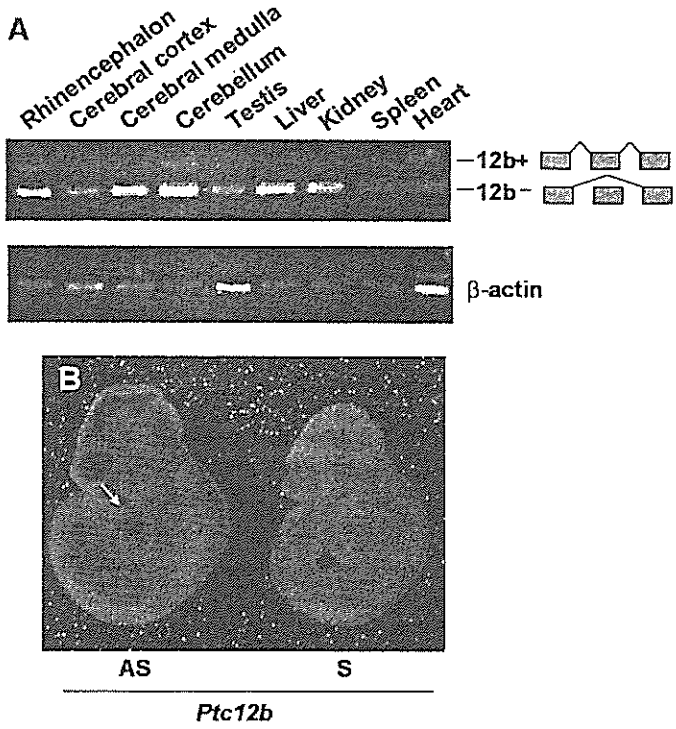

Fig. 2. Tissue-specific expression of *Ptc12b* in mice. (A) Total RNAs obtained from a panel of mouse tissues were subjected to RT-PCR with β-actin as an internal control. A forward primer for exon 11 and a reverse primer for exon 14 were synthesized and used for RT-PCR. All tissues were obtained from a 1-month-old mouse. (B) Whole mount *in situ* hybridization on mouse embryos. Digoxigenin-labeled RNA probes were synthesized in both orientations, sense (S) and antisense (AS), and used on embryos at E10.5. The arrow indicates the position of the heart.

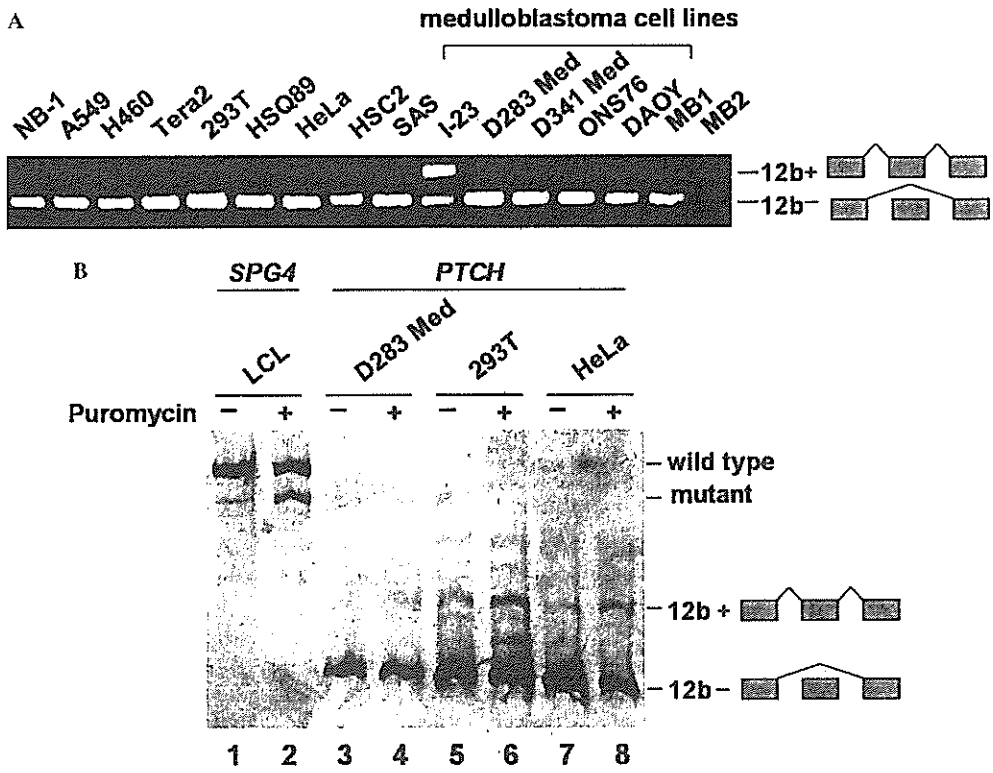

Fig. 3. Expression of exon12b in human cell lines and medulloblastomas. (A) RT-PCR analysis was performed using specific primers for exon 11 and exon 13. RNAs extracted from various cell lines and medulloblastoma samples (MB1, MB2) were used as templates. (B) *PTCH12b* is subjected to NMD to a small extent. Cell lines indicated at the top were grown in the presence or absence of 100 μg/ml puromycin for 6 h. Total RNA was extracted and subjected to RT-PCR. The RT-PCR products were run on a 3.5% polyacrylamide gel to emphasize the difference in size between transcripts from wild type allele and mutant allele of the *SPG4* gene.

PTCH12b isoform undergoes NMD to a small extent

It is known that spliced transcripts with PTCs, such as *Ptc12b* or *PTCH12b*, can potentially activate transcript degradation via the process of nonsense-mediated mRNA decay (NMD) [18]. NMD is important for the removal of PTC-containing transcripts encoding nonfunctional or potentially dominant negative proteins. In order to investigate this possibility, D283 Med, 293T, and HeLa cells, which express barely detectable levels of *PTCH12b*, were cultured in the presence or absence of an NMD inhibitor, puromycin, and subjected to RT-PCR as described above. A lymphoblastoid cell line (LCL) established from a patient in which a PTC is created due to the mutation in the *SPG4* gene (unpublished data by H. U., K. F. and T. M.) was employed as a positive control for NMD. Compared with the positive control where the levels of the transcript containing PTC were markedly increased upon the treatment with puromycin (Fig. 3B, lane 2, mutant), the transcripts of *PTCH12b* were only marginally elevated upon the treatment (Fig. 3B, lanes 4, 6, and 8). Similar results were obtained using another NMD inhibitor, cycloheximide (data not shown). This implies that this isoform undergoes NMD to a limited extent and is already expressed at low abundance independently of NMD in most tissues.

PTCH12b functions as a dominant negative isoform

We performed a functional analysis of PTCH12b using a GLI-responsive luciferase reporter in I-23 medulloblastoma cells. The binding of Shh to its receptor activates a signaling cascade that ultimately leads to an increased activity of the GLI family of transcription factors. The luciferase activities were suppressed when I-23 cells were transfected with plasmids for PTCH, but not with a plasmid for PTCH12b, consistent with PTCH being a suppressive component of the Shh receptor. This also implies that there is a basal level of leakage activity of Smo that excess PTCH prevents in the apparent absence of Shh. However, this suppression by PTCH was relieved when cotransfected with a plasmid for PTCH12b (Fig. 4A). Taken together, these results imply that the PTCH12b protein has a dominant negative effect on PTCH. In order to investigate the subcellular localizations, PTCH12b, as well as PTCH, both tagged with myc at their N-terminal ends, was expressed in HeLa cells and stained with an anti-myc antibody followed by confocal microscopy. PTCH was mainly localized in cytoplasmic vesicular structures as previously reported [19], and no significant difference in localization was observed between PTCH and PTCH12b (Fig. 4B and C). Therefore, it is unlikely that the dominant negative function of PTCH12b is due to its subcellular localization dis-

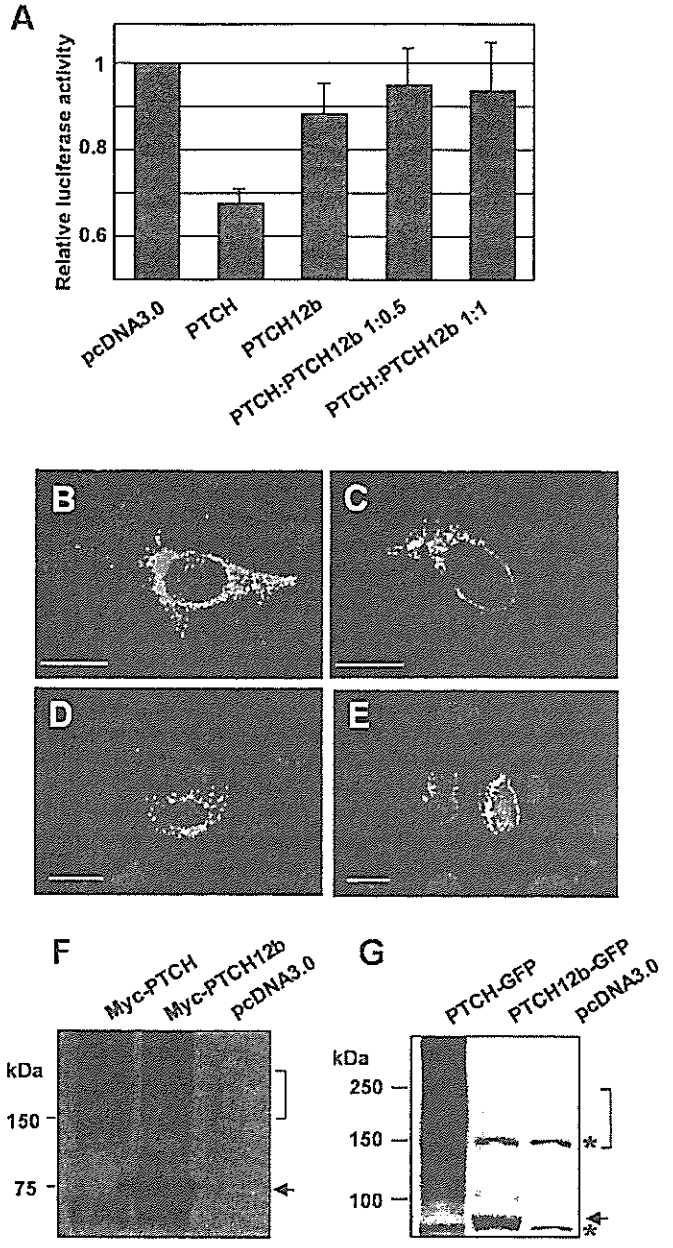

Fig. 4. Functional analysis of *PTCH12b*. (A) I-23 cells were transfected with various combinations of expression plasmids indicated at the bottom, together with a construct for a GLI-responsive luciferase reporter, 8 × GLI-Luc. Twenty-four hours after the transfection, cells were harvested and subjected to a luciferase assay. Shown are the representative data obtained in two independent experiments with triplicates in each experiment. (B–E) Subcellular localization of PTCH proteins. The expression patterns of myc-tagged (B and C) and EGFP-tagged (D and E) PTCH (B and D) or PTCH12b (C and E) in HeLa cells were examined using confocal microscopy. The nuclei were counterstained with Hoechst33342. Bar, 20 μm. (F and G) Western blotting was performed using protein samples obtained from the HeLa cells described above. Anti-c-myc (F) and anti-GFP (G) antibodies were used as a primary antibody. Asterisks indicate non-specific bands.

tinct from PTCH. Similar results were obtained when the both isoforms tagged with enhanced green fluorescent protein (EGFP) at their C-terminal ends were expressed (Fig. 4D and E). Comparative levels of protein expressions of both PTCH and PTCH12b with expected sizes were confirmed by Western blotting (Fig. 4F and G), indicating that the stability of the PTCH12b protein is similar to that of PTCH.

Discussion

Exon 12b in the human *PTCH* gene is conserved in mice and expressed in a brain- and heart-specific manner in both species. According to a recent report by Pan et al., alternative exons with the potential to introduce PTCs upon exon inclusion are not usually conserved between humans and mice [20], suggesting some biological significance of exon 12b.

The precise mechanism of how Ptc12b/PTCH12b functions as a dominant negative isoform remains to be elucidated. Recently, two mutant forms of the Ptc1 protein, G509V and 1130X, have been reported to be dominant negative forms, at least in *Drosophila* [21–23]. Whereas 1130X accumulated strongly along the plasma membrane, G509V and wild-type Ptc1 protein localized mainly in the cytoplasmic vesicles, indicating that their mode of action is different [22,23]. Our isoform localized in the cytoplasm. We failed to detect a significant difference in the subcellular localization between PTCH and PTCH12b. It would be interesting to see the *in vivo* function of Ptc12b/PTCH12b using animal models.

The important question would be whether truncated PTCH proteins generally function in a dominant negative manner, because most of the mutations found in patients with NBCCS lead to the truncation of the PTCH protein due to the frameshift or nonsense mutations [24,25]. $Ptc1^{-/-}$ mice are embryonic lethal due to the failure of neural tube closure and abnormal development of the heart [26]. Therefore, if truncated PTCH proteins are generally dominant negatives, then the patients with NBCCS should have a phenotype similar to that of $Ptc1^{-/-}$ mice, which is not the case. There are at least three explanations regarding this issue. First, mRNA with a frameshift or nonsense mutation may be expressed less than the wild type through NMD-dependent and/or independent mechanisms [20]. Second, at least truncated proteins with a large C-terminal deletion are unlikely to function as a dominant negative. Third, the sensitivity to the perturbation of SHH signaling may be species dependent. For example, mutations in the *SHH* gene are found in some of the children with autosomal dominant holoprosencephaly [27,28], whereas a phenotype resembling human holoprosencephaly is found in $Shh^{-/-}$ mice, but not in $Shh^{+/-}$ mice [29].

Synthesis of large amounts of C-terminally truncated polypeptides encoded by PTC-containing mRNA is avoided by a splicing- and translation-dependent NMD. Therefore, we wondered why *Ptc12b/PTCH12b* is expressed at high levels in certain tissues. Since NMD inhibition resulted in a limited amount of increase in expression of *PTCH12b*, we concluded that this isoform is already present at low levels independently from NMD in most tissues,

and that in the brain and some of the medulloblastomas it is abundantly expressed through a mechanism distinct from the inhibition of NMD. This conclusion is not surprising considering the recent report that only a fraction of PTC-introducing AS events are significantly regulated by NMD [20].

Although a relatively low frequency (10–20%) of sporadic medulloblastomas carry *PTCH* mutations [8], microarray analysis revealed that almost all medulloblastomas with desmoplastic histology are characterized by activation of the SHH signaling pathway [30]. Given the dominant negative function of PTCH12b and the detection of this isoform in the cerebellum and medulloblastoma, it is intriguing to speculate that *PTCH12b* plays an important role in the development of medulloblastoma. In our experiment, 1 out of 5 medulloblastoma cell lines expressed this isoform, whereas 2 out of 2 medulloblastoma tissues expressed this isoform. This may reflect the recent report that Shh activity is down-regulated in cultured medulloblastoma cells [31]. Tumor-specific AS is not a rare event based on a genome-wide computational screen [32]. However, the functional significance of respective protein isoforms generated by these ASs in oncogenesis has yet to be clarified. In NBCCS patients, 65 out of 132 *PTCH* mutations (49%) are localized in the second half of the protein (exon 13 or more downstream). Interestingly, in sporadic medulloblastomas, 16 out of 23 mutations (70%) are found in this region [33], implying that the gene structure encoding *PTCH12b* is more frequently preserved in sporadic medulloblastomas. Although more cases are needed to be investigated, consideration of not only the total expression levels of *PTCH* but also the expression of this particular *PTCH* isoform may help classify medulloblastomas and predict the clinical outcome of the children with medulloblastoma. Lastly, it should be noted that 3% of the individuals with NBCCS are known to have cardiac fibromas [34] and the heart is another tissue where *PTCH12b* is expressed.

Acknowledgments

We thank Mayu Yamazaki-Inoue for her technical support, and Kayoko Saito for preparing the manuscript. This work was supported by the Naito Foundation and Grants for Cancer Research from the Ministry of Health, Labour and Welfare and a Grant-in-Aid for Scientific Research and the Budget for Nuclear Research from the Ministry of Education, Culture, Sports, Science and Technology.

References

[1] P.W. Ingham, A.P. McMahon, Hedgehog signaling in animal development: paradigms and principles, Genes Dev. 15 (2001) 3059–3087.

[2] R.L. Johnson, A.L. Rothman, J. Xie, L.V. Goodrich, J.W. Bare, J.M. Bonifas, A.G. Quinn, R.M. Myers, D.R. Cox, E.H. Epstein Jr., M.P. Scott, Human homolog of *patched*, a candidate gene for the basal cell nevus syndrome, Science 272 (1996) 1668–1671.

[3] H. Hahn, C. Wicking, P.G. Zaphiropoulous, M.R. Gailani, S. Shanley, A. Chidambaram, I. Vorechovsky, E. Holmberg, A.B. Unden, S. Gillies, K. Negus, I. Smyth, C. Pressman, D.J. Leffell, B. Gerrard, A.M. Goldstein, M. Dean, R. Toftgard, G. Chenevix-Trench, B. Wainwright, A.E. Bale, Mutations of the human homolog of *Drosophila patched* in the nevoid basal cell carcinoma syndrome, Cell 85 (1996) 841–851.

[4] R.J. Gorlin, Nevoid basal-cell carcinoma syndrome, Medicine (Baltimore) 66 (1987) 98–113.

[5] J.E. Ming, M.E. Kaupas, E. Roessler, H.G. Brunner, M. Golabi, M. Tekin, R.F. Stratton, E. Sujansky, S.J. Bale, M. Muenke, Mutations in PATCHED-1, the receptor for SONIC HEDGEHOG, are associated with holoprosencephaly, Hum. Genet. 110 (2002) 297–301.

[6] M.R. Gailani, M. Stahle-Backdahl, D.J. Leffell, M. Glynn, P.G. Zaphiropoulos, C. Pressman, A.B. Undén, M. Dean, D.E. Brash, A.E. Bale, R. Toftgård, The role of the human homologue of *Drosophila patched* in sporadic basal cell carcinomas, Nat. Genet. 14 (1996) 78–81.

[7] A.B. Undén, E. Holmberg, B. Lundh-Rozell, M. Stahle-Backdahl, P.G. Zaphiropoulos, R. Toftgård, I. Vorechovsky, Mutations in the human homologue of *Drosophila patched* (*PTCH*) in basal cell carcinomas and the Gorlin syndrome: different in vivo mechanisms of PTCH inactivation, Cancer Res. 56 (1996) 4562–4565.

[8] C. Raffel, R.B. Jenkins, L. Frederick, D. Hebrink, B. Alderete, D.W. Fults, C.D. James, Sporadic medulloblastomas contain *PTCH* mutations, Cancer Res. 57 (1997) 842–845.

[9] P. Kogerman, D. Krause, F. Rahnama, L. Kogerman, A.B. Undén, P.G. Zaphiropoulos, R. Toftgård, Alternative first exons of *PTCH1* are differentially regulated *in vivo* and may confer different functions to the PTCH1 protein, Oncogene 21 (2002) 6007–6016.

[10] T. Shimokawa, F. Rahnama, P.G. Zaphiropoulos, A novel first exon of the *Patched1* gene is upregulated by Hedgehog signaling resulting in a protein with pathway inhibitory functions, FEBS Lett. 578 (2004) 157–162.

[11] K. Nagao, M. Toyoda, K. Takeuchi-Inoue, K. Fujii, M. Yamada, T. Miyashita, Identification and characterization of multiple isoforms of a murine and human tumor suppressor, *patched*, having distinct first exons, Genomics 85 (2005) 462–471.

[12] K. Nagao, N. Togawa, K. Fujii, H. Uchikawa, Y. Kohno, M. Yamada, T. Miyashita, Detecting tissue-specific alternative splicing and disease-associated aberrant splicing of the *PTCH* gene with exon junction microarrays, Hum. Mol. Genet. 14 (2005) 3379–3388.

[13] T. Miyashita, Y. Okamura-Oho, Y. Mito, S. Nagafuchi, M. Yamada, Dentatorubral pallidoluysian atrophy (DRPLA) protein is cleaved by caspase-3 during apoptosis, J. Biol. Chem. 272 (1997) 29238–29242.

[14] M. U, T. Miyashita, Y. Ohtsuka, Y. Okamura-Oho, Y. Shikama, M. Yamada, Extended polyglutamine selectively interacts with caspase-8 and -10 in nuclear aggregates, Cell Death Differ. 8 (2001) 377–386.

[15] Y. Shikama, M. U, T. Miyashita, M. Yamada, Comprehensive studies on subcellular localizations and cell death-inducing activities of eight GFP-tagged apoptosis-related caspases, Exp. Cell Res. 264 (2001) 315–325.

[16] P.E. Kuwabara, M. Labouesse, The sterol-sensing domain: multiple families, a unique role? Trends Genet. 18 (2002) 193–201.

[17] S. Minovitsky, S.L. Gee, S. Schokrpur, I. Dubchak, J.G. Conboy, The splicing regulatory element, UGCAUG, is phylogenetically and spatially conserved in introns that flank tissue-specific alternative exons, Nucleic Acids Res. 33 (2005) 714–724.

[18] J.A. Holbrook, G. Neu-Yilik, M.W. Hentze, A.E. Kulozik, Nonsense-mediated decay approaches the clinic, Nat. Genet. 36 (2004) 801–808.

[19] J. Taipale, M.K. Cooper, T. Maiti, P.A. Beachy, Patched acts catalytically to suppress the activity of Smoothened, Nature 418 (2002) 892–896.

[20] Q. Pan, A.L. Saltzman, Y.K. Kim, C. Misquitta, O. Shai, L.E. Maquat, B.J. Frey, B.J. Blencowe, Quantitative microarray profiling provides evidence against widespread coupling of alternative splicing

with nonsense-mediated mRNA decay to control gene expression, Genes Dev. 20 (2006) 153–158.
[21] R.L. Johnson, L. Milenkovic, M.P. Scott, In vivo functions of the patched protein: requirement of the C terminus for target gene inactivation but not Hedgehog sequestration, Mol. Cell 6 (2000) 467–478.
[22] A.J. Zhu, L. Zheng, K. Suyama, M.P. Scott, Altered localization of *Drosophila* Smoothened protein activates Hedgehog signal transduction, Genes Dev. 17 (2003) 1240–1252.
[23] G.R. Hime, H. Lada, M.J. Fietz, S. Gillies, A. Passmore, C. Wicking, B.J. Wainwright, Functional analysis in *Drosophila* indicates that the NBCCS/PTCH1 mutation G509V results in activation of smoothened through a dominant-negative mechanism, Dev. Dyn. 229 (2004) 780–790.
[24] C. Wicking, S. Shanley, I. Smyth, S. Gillies, K. Negus, S. Graham, G. Suthers, N. Haites, M. Edwards, B. Wainwright, G. Chenevix-Trench, Most germ-line mutations in the nevoid basal cell carcinoma syndrome lead to a premature termination of the PATCHED protein, and no genotype-phenotype correlations are evident, Am. J. Hum. Genet. 60 (1997) 21–26.
[25] K. Fujii, Y. Kohno, K. Sugita, M. Nakamura, Y. Moroi, K. Urabe, M. Furue, M. Yamada, T. Miyashita, Mutations in the human homologue of *Drosophila patched* in Japanese nevoid basal cell carcinoma syndrome patients, Hum. Mutat. 21 (2003) 451–452.
[26] L.V. Goodrich, L. Milenković, K.M. Higgins, M.P. Scott, Altered neural cell fates and medulloblastoma in mouse patched mutants, Science 277 (1997) 1109–1113.
[27] E. Belloni, M. Muenke, E. Roessler, G. Traverso, J. Siegel-Bartelt, A. Frumkin, H.F. Mitchell, H. Donis-Keller, C. Helms, A.V. Hing, H.H. Heng, B. Koop, D. Martindale, J.M. Rommens, L.C. Tsui, S.W. Scherer, Identification of Sonic hedgehog as a candidate gene responsible for holoprosencephaly, Nat. Genet. 14 (1996) 353–356.
[28] E. Roessler, E. Belloni, K. Gaudenz, P. Jay, P. Berta, S.W. Scherer, L.C. Tsui, M. Muenke, Mutations in the human Sonic Hedgehog gene cause holoprosencephaly, Nat. Genet. 14 (1996) 357–360.
[29] C. Chiang, Y. Litingtung, E. Lee, K.E. Young, J.L. Corden, H. Westphal, P.A. Beachy, Cyclopia and defective axial patterning in mice lacking Sonic hedgehog gene function, Nature 383 (1996) 407–413.
[30] S.L. Pomeroy, P. Tamayo, M. Gaasenbeek, L.M. Sturla, M. Angelo, M.E. McLaughlin, J.Y. Kim, L.C. Goumnerova, P.M. Black, C. Lau, J.C. Allen, D. Zagzag, J.M. Olson, T. Curran, C. Wetmore, J.A. Biegel, T. Poggio, S. Mukherjee, R. Rifkin, A. Califano, G. Stolovitzky, D.N. Louis, J.P. Mesirov, E.S. Lander, T.R. Golub, Prediction of central nervous system embryonal tumour outcome based on gene expression, Nature 415 (2002) 436–442.
[31] K. Sasai, J.T. Romer, Y. Lee, D. Finkelstein, C. Fuller, P.J. McKinnon, T. Curran, Shh pathway activity is down-regulated in cultured medulloblastoma cells: implications for preclinical studies, Cancer Res. 66 (2006) 4215–4222.
[32] Z. Wang, H.S. Lo, H. Yang, S. Gere, Y. Hu, K.H. Buetow, M.P. Lee, Computational analysis and experimental validation of tumor-associated alternative RNA splicing in human cancer, Cancer Res. 63 (2003) 655–657.
[33] E. Lindström, T. Shimokawa, R. Toftgård, P.G. Zaphiropoulos, PTCH mutations: distribution and analyses, Hum. Mutat. 27 (2006) 215–219.
[34] D.G. Evans, E.J. Ladusans, S. Rimmer, L.D. Burnell, N. Thakker, P.A. Farndon, Complications of the naevoid basal cell carcinoma syndrome: results of a population based study, J. Med. Genet. 30 (1993) 460–464.

Available online at www.sciencedirect.com
SCIENCE DIRECT
Gene 366 (2006) 77–86
GENE
SECTION
FUNCTIONAL GENOMICS
www.elsevier.com/locate/gene

Comparative analyses of genomic imprinting and CpG island-methylation in mouse *Murr1* and human *MURR1* loci revealed a putative imprinting control region in mice

Zhongming Zhang [a], Keiichiro Joh [a], Hitomi Yatsuki [a], Youdong Wang [a,1], Yuji Arai [c], Hidenobu Soejima [a], Ken Higashimoto [a], Tsuyoshi Iwasaka [b], Tsunehiro Mukai [a,*]

[a] *Department of Biomolecular Sciences, Faculty of Medicine, Saga University, Saga 849-8501, Japan*
[b] *Department of Obstetrics and Gynecology, Faculty of Medicine, Saga University, Saga 849-8501, Japan*
[c] *Department of Bioscience, National Cardiovascular Center Research Institute, Osaka 565-8565, Japan*

Received 13 June 2005; accepted 13 August 2005
Available online 21 November 2005
Received by T. Sekiya

Abstract

Human *MURR1* is an orthologue of mouse *Murr1* gene, which was previously reported to be imprinted only in adult brain with a maternal allele-predominant expression and to contain another imprinted gene, *U2af1-rs1*, in the first intron. Human *MURR1* was found not to harbor the *U2af1-rs1* orthologue and to be expressed biallelically in tissues, including adult brain. Three genes identified around *Murr1* and their orthologues around *MURR1* were expressed biallelically. These findings suggest that the mouse imprinting locus is limited to a small region and the introduction of *U2af1-rs1* in mouse causes the imprinting of this locus. The CpG island (CGI) at *U2af1-rs1* with maternal methylation was the only differentially methylated region among CGIs found in these loci. Detailed methylation analyses of the *U2af1-rs1* CGI in germ cells led to identification of a region with oocyte-specific methylation. These results suggest that this region is the imprinting control region of the *Murr1/U2af1-rs1* locus in mouse.

Keywords: Genomic imprinting; CpG island; Differentially methylated region; Gametic methylation; *Murr1*; *U2af1-rs1*

1. Introduction

Differing from the expression of most genes, imprinted genes show allele-specific expression according to their parental origin (Reik and Walter, 2001). To date, more than 70 imprinted genes have been reported in mouse, more than half of which have human imprinted orthologues (http://cancer.otago.ac.nz/IGC/Web/home.html). Imprinted genes tend to cluster in subchromosomal domains, called imprinting domains. It has been indicated that imprinted genes in a domain are coordinately regulated by long-range *cis*-acting regulatory elements called an imprinting control region (ICR). For example, seven imprinted genes located within the approximately 500 kb region of *Kip2/Lit1* imprinting subdomain on mouse chromosome 7F4/F5 have their allelic expressions regulated by the ICR called *KvDMR1* (or *DMR-Lit1*) (Smilinich et al., 1999; Yatsuki et al., 2002; Fitzpatrick et al., 2002). Clustered organizations of imprinted genes are conserved between mouse and human in many imprinting domains (Reik and Walter, 2001). Many imprinted genes are linked to a differentially methylated region (DMR) carrying parental origin-specific methylation. DMRs are

Abbreviations: CGI, CpG island; DMR, differentially methylated region; COBRA, combined bisulfite restriction analysis; ICR, imprinting control region; RFLP, restriction-fragment length polymorphism; RT-PCR, reverse transcription-PCR; SNP, single nucleotide polymorphism; BPF1, hybrid F1 mouse from the cross between female C57BL/6 and male PWK; PBF1, hybrid F1 mouse from the cross between female PWK and male C57BL/6.

* Corresponding author. Division of Molecular Biology and Genetics, Department of Biomolecular Sciences, Faculty of Medicine, Saga University, 5-1-1 Nabeshima, Saga 849-8501, Japan. Tel.: +81 952 34 2260; fax: +81 952 34 2067.
E-mail address: mukait@med.saga-u.ac.jp (T. Mukai).
[1] Present address: Department of Ophthalmology, the First Clinical College and the First Affiliated Hospital, China Medical University, Heping District, Shenyang, Liaoning Province 110001, China.

0378-1119/$ - see front matter © 2005 Elsevier B.V. All rights reserved.
doi:10.1016/j.gene.2005.08.020

generally CpG rich and often fulfill the criteria for CpG islands (CGI). A DMR, whose methylation is established during gametogenesis, is a strong candidate for the imprint of parental origin of an allele. Such a DMR is often recognized to function as the ICR for the allelic expression of the linked imprinted gene (s) (Fitzpatrick et al., 2002; Wutz et al., 1997; Thorvaldsen et al., 1998).

Mouse *Murr1* is located on chromosome 11 A3.2 and is imprinted only in adult brain with a maternal allele-predominant expression (Nabetani et al., 1997; Wang et al., 2004). In the first intron of *Murr1* there exists an antisense-oriented imprinted gene *U2af1-rs1*, which is transcribed exclusively from the paternal allele (Fig. 1A) (Nabetani et al., 1997; Hatada et al., 1993; Tada et al., 1994). It is proposed that the imprinting of *Murr1* results from transcriptional interference by the *U2af1-rs1* gene (Wang et al., 2004). According to this model, the imprinting of *U2af1-rs1* is the primary event and that of *Murr1* is caused by the paternal expression of *U2af1-rs1*. Nothing is, however, known about the imprinting statuses of adjacent genes. It is very important to know if *Murr1* and *U2af1-rs1* genes are isolated imprinted genes or members in a large imprinted domain, implying a connected imprinting mechanism. It is also important to analyze the human orthologous genes in their syntenic region because comparative genomics has been recognized as a useful procedure to identify *cis*-acting regulatory region in the genome.

In this study, we analyzed the imprinting status of the genes and methylation status of CGIs in a large region around mouse *Murr1* and in the human syntenic region. The results indicated that *Murr1* and *U2af1-rs1* were the only genes imprinted in this mouse chromosomal region and that there was no imprinted gene in the human syntenic region. Methylation analyses led us to identify an oocyte-specifically methylated region linked to *U2af1-rs1* as a strong candidate for the ICR of the imprinted genes.

2. Materials and methods

2.1. Cloning and analysis of human MURR1 cDNA

The human testis 5′-STRETCH PLUS cDNA library, #HL50335 (Clontech Lab. USA), was screened with a radioactively labeled probe prepared from a partial *MURR1* cDNA clone isolated by Nabetani et al. (1997). Positive clones were isolated according to the supplier's protocol, and their cDNA inserts were sequenced. The sequencing was performed using a BigDye Terminator Kit, followed by analysis on an ABI PRISM™ 310 Genetic Analyzer. To obtain the full-length *MURR1* cDNA sequence, 5′-RACE procedure (TaKaRa Biomedicals Co., Japan) was performed with human kidney poly(A)$^+$ RNA according to the manufacturer's protocol. The RACE-PCR products were subsequently cloned in pT7 Blue T-Vectors (TaKaRa) and sequenced.

2.2. Isolation of genomic DNA and RNA from mouse and human tissues

QIAamp Tissue Kit (Qiagen, Germany) was used to isolate genomic DNA from mouse and human tissues. Total RNA was isolated with an ISOGEN Kit (Nippon Gene Co., Japan) and treated with RNase-free DNase I (Boehringer Mannheim, Germany).

Human adult brains (17 to 36 years, 15 males and 5 females) and fetal tissues (54 to 115 days of pregnancy) were obtained from the Brain and Tissue Bank for Developmental Disorder at the University of Maryland and from the Fetal Tissue Bank at the Birth Defect Research Laboratory at the University of Washington, respectively. We have conducted our research with these human tissues under the approval of the Ethical Committee for Research on Human Materials of our university.

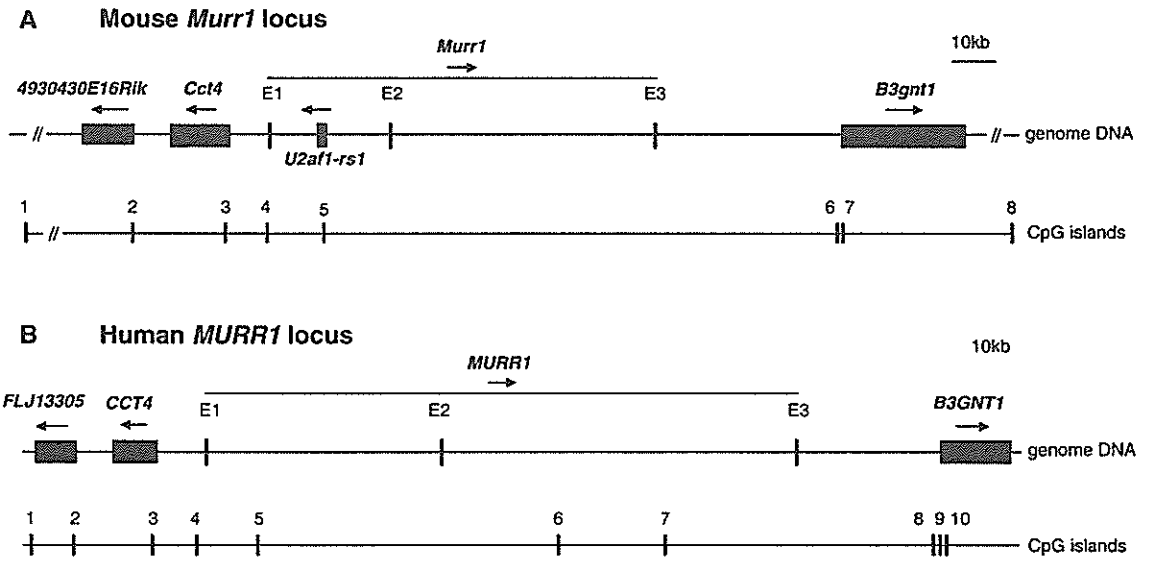

Fig. 1. Schematic physical map of mouse *Murr1* locus on chromosome 11 A3.2 and human *MURR1* locus on chromosome 2p15. The genes or exons (for *Murr1* and *MURR1*) and CpG islands are shown with solid boxes and vertical bars, respectively. Their positions are based on previously published data and on our identified results. Horizontal arrows indicate the transcriptional direction of the genes.

2.3. Analyses of allelic expression of human MURR1 gene

Two SNPs were identified in exon 3 by sequencing of PCR-amplification products of the genomic region with a pair of primers. PCR reactions were performed in a 10-μl volume containing ~100 ng template DNA, 0.5 pM of each primer, 0.2 mM dNTPs, and 0.5 unit of LA Taq polymerase (TaKaRa) in 1× LA-PCR buffer with 2.0 mM $MgCl_2$. The amplification reaction was in 35 cycles of 96 °C for 30 s, at 60.5 °C for 30 s, and at 72 °C for 30 s. This PCR reaction mixture and reaction condition was used as a standard in all other PCR and RT-PCR experiments in this paper unless stated otherwise. The information of the primers used in PCRs is available from the authors, if it is not presented in the text.

Using DNA-free total RNA, reverse transcription was performed to synthesize single-stranded cDNA according to the manufacturer's protocol (RNA PCR Kit AMV, TaKaRa). The primers 5′-TGGAGGCATTCTTGACTGCT and 5′-TTGACTGAATGCGAGGATTT (annealed at 58.5 °C) were used in RT-PCR. The PCR products were recovered and analyzed for one SNP by digestion with the restriction endonuclease *Tth111*I (RFLP analyses) and by sequencings. Another SNP was in the *Sdu*I recognition site and was analyzed by the same methods.

2.4. Analyses of allelic expression of genes surrounding mouse Murr1 and human MURR1

DNA polymorphisms in the six genes were identified by sequencing of PCR products of genomic sequences in mouse and human individuals.

The following primers were used in RT-PCR to amplify cDNA regions carrying SNPs: 5′-CTGGAGGTGTCCCTAGACAA/5′-ACAAACTCTGCGTCTGGACA (63.5 °C) for *B3gnt1*, 5′-GCCAACTGGAAGACAATGTC/5′-GGCCTGAATCCCATTTCTAC (63.5 °C) for *Cct4*, 5′-ATGGGATCAGCGATTCGTCT/5′-CTCTGCTTGACTAGATCCTC (62 °C) for *Rik*, 5′-CTCAGTTGCAGAGTGCTCAT/5′-GAATTCCACAACTGACAACTG (61 °C) for *B3GNT1*, 5′-AGTCAGTGCTCTGACTCTTG/5′-GAGGTGCCACTTGGATCATT (62 °C) for *CCT4*, and 5′-TTTCACCATGTTGGCCAGAT/5′-GTCCTCATAGCTTATCGGTG (61 °C) for *FLJ*. The PCR products were analyzed by direct sequencing or RFLP analyses with restriction nucleases, *Nhe*I for *B3gnt1*, *Hinc*II for *Cct4*, and *Bsm*AI for *FLJ*. In the analysis of *FLJ*, hot-stop RT-PCR was performed as described (Wang et al., 2004; Uejima et al., 2000). Labeled PCR product was recovered, digested with *Bsm*AI, and electrophoresed. Intensity of electrophoretic bands was measured using the Bio Image Analyzer BAS2000 (Fujifilm, Japan).

2.5. Analyses of methylation statuses of CpG islands around mouse Murr1/U2af1-rs1 and human MURR1 genes

Genomic sequence data of the mouse locus was obtained under accession no. NT_039515.2. Human genomic sequence data was obtained under accession nos. AC107081, AC116652, and AC018462. To identify CGIs, the GRAIL and CpG percent analyses were performed on the websites, http://compbio.ornl.gov/Grail-1.3/ and http://www.nih.go.jp/yoken/genebank/cpg_per.html. Hot-stop COBRA procedure (Uejima et al., 2000; Xiong and Laird, 1997) was carried out as follows.

Sodium bisulfite treatment of genome DNA was carried out as described (Paulin et al., 1998) with some modifications (Yatsuki et al., 2002). Nested or semi-nested PCR amplifications were performed with the primer pairs for each of the mouse and human CGIs. The first PCR was performed with bisulfite-treated DNA, 1 unit of LA Taq polymerase, elongation for 45 s, in 40 cycles. The second PCR was done using 1 μl of 50-times diluted first PCR products. An additional amplification cycle was done with one γ-^{32}P labeled primer from two of the second PCR pair-primers. PCR products were recovered, digested by restriction nucleases, and electrophoresed. The radioactive intensity of each band was measured by BAS2000. The nucleases used were *Rsa*I, *Acc*II, *Acy*I, *Hinf*I, *Acc*II, *Acc*II, *Acc*I, and *Acc*II for mouse CGI1 through CGI8; *Taq*I, *Acy*I, *Rsa*I, *Taq*I, *Taq*I, *Hinf*I, *Hha*I, *Hha*I, *Acy*I, and *Rsa*I for human CGI1 through CGI10, respectively (Fig. 4). Another nuclease was used for each of the CGIs to confirm the results.

2.6. Analysis of methylation status of U2af1-rs1 CpG island (CGI5) in mouse adult somatic tissues and germ cells

Preparation of sperm and oocyte, isolation of DNA, and sodium bisulfite treatment of the DNA were as described previously (Yatsuki et al., 2002). Oocytes were prepared by picking them up one by one with micropipettes under a microscope to avoid somatic cell contamination. PCRs were carried out with the primer pairs 5′-GGAAGGTGAGTTGTTAGTAT/5′-ACCAACCTATACAATTACTA followed by GTGTTTTGTAGTGAGATAAG/5′-ATAACACAACTAACCTATAC for region a, and 5′-GTATAGGTTAGTTGTGTTAT/5′-ACCTACCTAAACAATCACCC (U2BS-R3) followed by 5′-TAGTAATTGTATAGGTTGGT/U2BS-R3 for region b. The second PCR products were cloned into pT7 blue vectors and sequenced. The SNPs between B6 and PWK in analyzed regions were used to distinguish the parental alleles.

3. Results and discussion

3.1. Characterization of the human MURR1 gene

We have previously reported the characterization of the mouse *Murr1* gene (Nabetani et al., 1997; Wang et al., 2004). The gene consists of three exons and contains *U2af1-rs1* gene in the first intron (Fig. 1A). *U2af1-rs1* is an intronless imprinted gene expressing exclusively from the paternal allele. *Murr1* is an adult brain-specific imprinted gene of maternal allele-predominant expression. It is expressed biallelically in other adult tissues and in embryonic and neonatal brains. It has been suggested that the imprinting of *Murr1* is caused by the paternal allele-specific expression of *U2af1-rs1* gene. To know if the imprinting is conserved for human orthologue, *MURR1*, we have analyzed the genomic organization and the expression of the gene.

Human *MURR1* was first reported by Nabetani et al. (1997) and is assigned on human chromosome 2p15 (accession no. D85433). We have obtained a nearly full cDNA sequence by cDNA cloning and 5′-RACE analyses. The sequence is 711 bp in length, excluding the poly A tail, and its longest ORF is 573 bp. This ORF encodes a protein of 190 amino acids and is considered functional, based on several observations. The first ATG initiation codon is accompanied with the Kozak consensus sequence (Kozak, 1987). Secondly, the ORF was functional when it was cloned in an expression vector and was introduced into cultured cells (data not shown). In addition, the ORF is highly homologous to the 567 bp ORF of mouse *Murr1* cDNA (accession no. D85430). The *MURR1* mRNA sequence we identified was deposited in the DDBJ database under accession no. AB178811.

By comparing the cDNA sequence with the published genomic sequence, human *MURR1* was revealed to consist of three exons similar to mouse *Murr1* (Fig. 1B). *U2AF1-RS1* and *U2AF1-RS2* genes have been reported to be the human orthologues of mouse *U2af1-rs1* but are mapped on chromosomes 5 and X, respectively. Previous reports indicated the absence of the homologous sequence of *U2af1-rs1* on human chromosome 2, where *MURR1* is located, by FISH analyses of human cells (Kitagawa et al., 1995) and by Southern blot analyses of genomic DNA from mouse cells carrying human chromosome 2 (Nabetani et al., 1997). To verify this notion, we analyzed overlapping human genomic clones in bacterial artificial chromosomes, which cover the *MURR1*. No sequence homologous to *U2AF1-RS1* was detected on these clones by Southern blotting with *U2AF1-RS1* (accession no. D49676) DNA as a probe. Besides this, a homology search of the published sequences of the genomic clones with *U2AF1-RS1* sequence failed to identify any homology (data not shown). These results indicate that human *MURR1* does not contain the *U2af1-rs1* orthologue (Fig. 1B). It was proposed that the intronless gene, *U2af1-rs1*, was formed by retro-transposition of its paralogous non-imprinted gene *U2af1-rs2*, located on the X chromosome after the divergence of mouse and human (Nabetani et al., 1997).

3.2. *MURR1* is ubiquitously and biallelically expressed in adult and fetal tissues

Northern blotting revealed that *MURR1* gene was expressed in all human adult tissues, with very high levels in liver, heart, skeletal muscle, and kidney (Fig. 2A). This ubiquitous expression was also detected in adult brains and fetal tissues by RT-PCR (Fig. 2B–D). The expression pattern is similar to that of the mouse homologue, *Murr1* (Wang et al., 2004).

Because mouse *Murr1* is imprinted only in adult brain, we have analyzed the allelic expression of human *MURR1* in adult and fetal brains, and additionally in other fetal tissues. Two SNPs were identified in exon 3 of *MURR1* in our human tissue samples, one of which was in a restriction site of *Tth111*I. Seven adult brains and eight fetuses heterozygous for the SNP in the *Tth111*I site were used for the analyses of allelic expression of *MURR1*. RT-PCR was performed on total RNAs of these informative samples, and the PCR products were subjected to RFLP analyses by *Tth111*I digestion. The *MURR1* gene was found to be expressed biallelically in all adult and fetal brains (Fig. 2B,C). Biallelic expression was also seen in the liver, kidney, heart, and muscle from one of the fetuses (Fig. 2D). These results were confirmed by direct sequencing of the PCR products and also

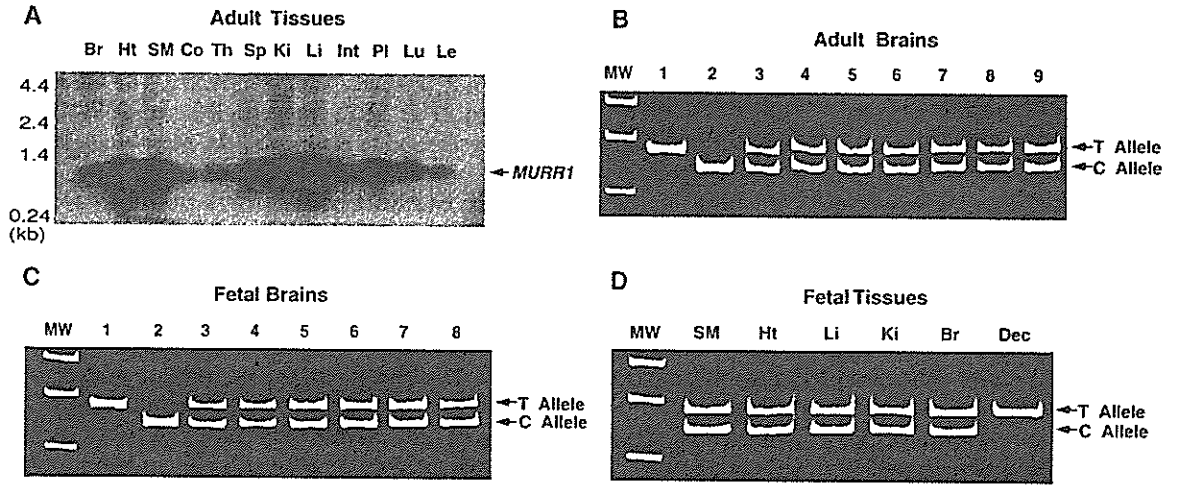

Fig. 2. Expression of human *MURR1* gene. (A) Northern blotting of *MURR1* on human adult tissues. Human 12-lane multiple tissue Northern blot (MTN™, Clontech) was hybridized with a ^{32}P-labeled *MURR1* cDNA probe. Tissues are brain (Br), heart (Ht), skeletal muscle (SM), colon (Co), thymus (Th), spleen (Sp), kidney (Ki), liver (Li), intestine (Int), placenta (Pl), lung (Lu), and peripheral blood leukocytes (Le). The positions of molecular weight markers are on the left side. The transcripts of *MURR1* were detected in all tissues, abundantly in heart, skeletal muscle, liver, and kidney. (B–D) Allelic expression of *MURR1* in human adult and fetal tissues. The polymorphic *Tth111*I site on the 478 bp RT-PCR fragment was used to distinguish the expression of two alleles by RFLP analyses in adult brains (B), fetal brains (C), and fetal tissues from one fetus (D). Fetal tissues in (D) are skeletal muscle (SM), heart (Ht), liver (Li), kidney (Ki), brain (Br), and decidua (Dec). Homozygous tissues for T or C allele were used as controls in lane 1 and 2 in (B, C), and decidua lane in (D). Control experiments without reverse transcriptase were performed and no PCR product was observed. *MURR1* showed biallelic expression in all the informative samples.

by analyses of another SNP (data not shown). These results indicate that human *MURR1* is imprinted neither in fetal brain nor in adult brain, thereby differing from adult brain-specific imprinting of mouse *Murr1*. We have proposed a transcriptional interference model for the maternal predominant-expression of *Murr1* (Wang et al., 2004). According to this model, transcription from the resident *U2af1-rs1* gene goes through the *Murr1* promoter. This paternal transcription may interfere with the binding of transcription factors to the promoter of *Murr1* and cause the reduction of the expression of the paternal allele of *Murr1*. The absence of *U2af1-rs1* orthologue in non-imprinted human *MURR1* gene is consistent with this model and can be supportive evidence for it.

3.3. Genes surrounding mouse Murr1 and human MURR1 are not imprinted

Allelic expressions of imprinted genes in a cluster are suggested to be regulated coordinately by a common regulatory mechanism (Reik and Walter, 2001). It is, therefore, very important to know the allelic expressions of the genes linked to an imprinted gene to elucidate its imprinting mechanism. Three genes have been mapped in the 500-kb genomic region, spanning from 217 kb upstream to 200 kb downstream of mouse *Murr1* (Fig. 1A). The *B3gnt1* gene (accession nos. AF092050 and BF467111) is located 40.2 kb downstream of *Murr1* and genes, *4930430E16Rik* (referred to as *Rik* in the text; accession no. BC026495) and *Cct4* (accession no. NM_009837), are located 31 kb and 8.3 kb upstream of *Murr1*, respectively (see the web site, Ensembl Mouse Genome Browser, http://www.ensembl.org/Mus_musculus/contigview; Fig. 1A).

SNPs, identified in each of the genes between mouse strains C57/BL6 and PWK, were used to investigate their allelic expressions in F_1 hybrid mice of the two strains. All of the genes showed biallelic expressions in embryo, placenta, neonate, and many adult tissues, including the brain (Fig. 3A–C). These results suggest that *Murr1* and *U2af1-rs1* are the only imprinted genes in this chromosomal region and that their imprinting is controlled by a locally operating mechanism, rather than the large imprinted domains such as the *Kip2/Lit1* locus (Yatsuki et al., 2002), and the *PWS/AS* locus (Perk et al., 2002). However, the analysis of more distant genes in this region may be necessary to confirm this conclusion.

It is also suggested that the human syntenic region may not be an imprinted locus because there is no orthologue of mouse imprinted gene, *U2af1-rs1*, and human *MURR1* is not imprinted. To confirm this idea, we have analyzed the allelic expression of genes neighboring human *MURR1*. We found three human orthologues for the mouse genes described above within the region spanning from 84 kb upstream to 90 kb downstream of *MURR1* by using the Ensembl Human Genome Browser (http://www.ensembl.org/Homo_sapiens/contigview; Fig. 1B). Analyses of their allelic expressions were performed mainly on adult and fetal brains, because mouse *Murr1* is imprinted in adult brain.

Analyses of genes *B3GNT1* (accession no. NM_006577) and *CCT4* (accession nos. AF026291 and AL555754) were performed by sequencing the RT-PCR products of RNAs from

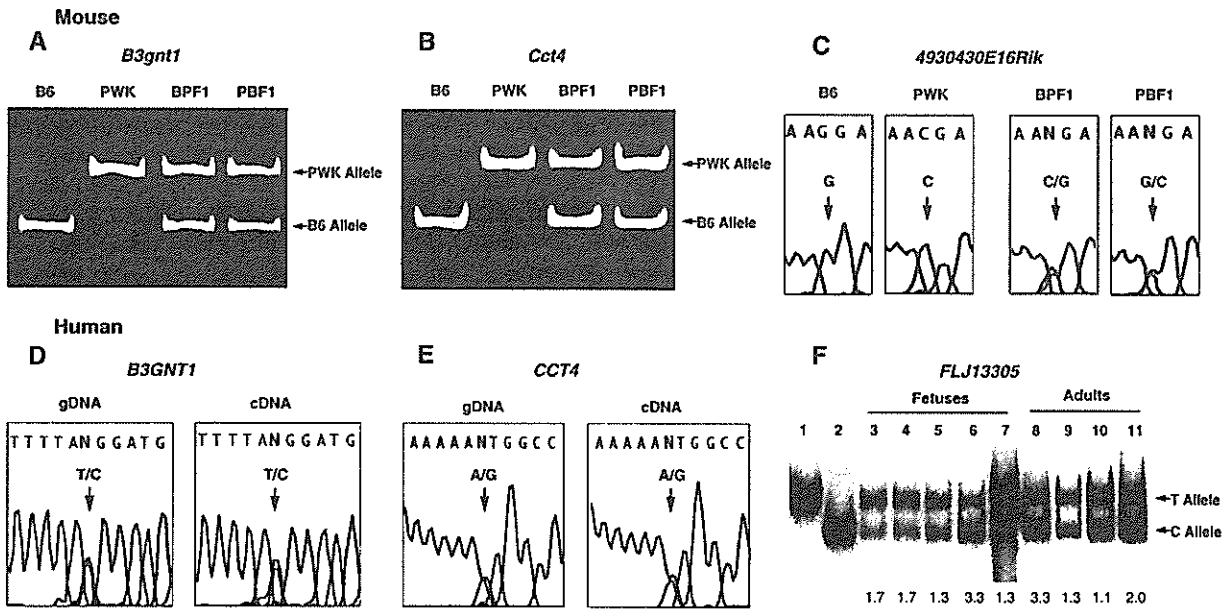

Fig. 3. Allelic expressions of the genes in mouse *Murr1* and human *MURR1* regions. (A, B, C) Analyses of three mouse genes were performed using adult brains of F1 hybrid mice (BPF_1 and PBF_1) and their parental strains, C57BL/6 (B6) and PWK. RT-PCR products were analyzed by direct RFLP analysis (A, B) or sequencing (C). (D, E, F) Analyses of three human genes were performed using brains heterozygous for one SNP of each gene. (D, E) RT-PCR products of *B3GNT1* and *CCT4* genes were analyzed by direct sequencing (cDNA). Results of sequencing of genomic DNAs at the SNP sites are also shown (gDNA). (F) Hot-stop RT-PCR products of the *FLJ* gene were subjected to RFLP analyses. Control RT-PCR without reverse transcriptase produced no product. Lanes 1 and 2, homozygous adult brains; lanes 3–7, heterozygous fetal brains; lanes 8–11, heterozygous adult brains. Ratio of intensities of the two bands is shown under each lane. RFLP analyses are described in Materials and methods. All three genes around mouse *Murr1* and their human orthologues were expressed biallelically.

informative tissues. Two adult brains and three fetuses were informative for an SNP identified in the *CCT4* gene. The gene was found to be expressed biallelically in all the brain samples and also in other tissues, including heart, kidney, liver, and muscle, from one informative fetus. The *B3GNTI* gene also showed biallelic expression in all the informative brain samples (five adults and four fetuses) and other fetal tissues. Representative results of adult brains are shown in Fig. 3D,E.

Hot-stop RT-PCR followed by RFLP analyses was used to analyze the allelic expression of *FLJ13305* gene (referred to as *FLJ* in the text; accession nos. AK023367 and XM_114287), the human orthologue of the mouse *Rik* gene. Four adults and eight fetuses were found to be informative for this gene. In addition to their brains, we have analyzed informative fetal tissues including eight kidneys, eight muscles, seven livers, six hearts, and two deciduas. Our analyses showed biallelic expression of the gene in all tissues, although some allelic variations of expression were seen in a few of the analyzed tissues (Fig. 3F and data not shown). The ratio of expression level of the two alleles ranged from 1.0 to 3.6 with an average of 1.8. Essentially the same results were obtained in three independent experiments. There was no specific fetal individual or specific tissue type that showed a high ratio. Variation of the allelic expression was randomly distributed among the tissue samples. It is, therefore, more plausible to conclude that *FLJ* gene is not imprinted and that the observed allelic differences are due to random allelic variation of gene expression. Recently, a large-scale analysis of allelic gene expression in human has shown that among the 602 genes, almost all were not imprinted, 326 (54%) showed at least twofold differential allelic expression in at least one of the seven individuals (Lo et al., 2003). Their study and the others demonstrated that allelic variation of gene expression is common in human and mouse (Knight, 2004; Yan et al., 2002; Cowles et al., 2002).

Considering our results, one can construct a hypothetical view of the formation of an imprinted locus in mouse. After the divergence of mouse and human, the intronless imprinted gene, *U2af1-rs1*, was formed within the ancestral non-imprinted *Murr1* gene by retro-transposition of a gene, probably the *U2af1-rs2* gene, in mouse. *U2af1-rs2* is a non-imprinted gene, mapped on the X chromosome, and orthologous to human *U2AF1-RS2* on the X chromosome (Yamaoka et al., 1995). The newly formed gene would have gained the maternal allele-specific methylation by unknown mechanisms with the methylation causing the imprinted paternal expression of the gene. This imprinted expression influenced only *Murr1* and resulted in maternal predominant-expression of the host gene, leaving the surrounding genes non-imprinted.

3.4. The CpG island of U2af1-rs1 gene is the only DMR in the mouse Murr1/U2af1-rs1 region, but no DMR exists in the human syntenic region

Many imprinted genes are linked to a differentially methylated region (DMR), which is methylated in an allele-specific manner, usually locates in a CpG island (CGI), and is considered to be involved in the allele-specific expression of linked imprinted gene(s). In the large imprinted chromosomal domain that includes many imprinted genes, their allele-specific expressions are coordinately regulated by a genomic region called ICR, which usually shows the methylation pattern as DMR (Reik and Walter, 2001; Constancia et al., 1998). These facts led us to analyze the methylation statuses of CGIs in the mouse *Murr1* region and in the human syntenic region to elucidate the imprinting mechanism of *Murr1* and *U2af1-rs1* genes.

Eight CGIs, designated as CGI1 to CGI8, were identified by computational search in the mouse genomic sequence of the 283 kb region, from 100 kb upstream to 100 kb downstream of *Murr1* (Fig. 1A). CGI1 is located approximately 86 kb upstream and CGI8 is 75 kb downstream from *Murr1*. Most CGIs, except for CGIs 1 and 8, were in the 5′ regions of the genes (Fig. 1A). The methylation status of each CGI was analyzed on the brain DNA of BPF_1 mouse by the hot-stop COBRA procedure. All the CGIs were unmethylated, except for CGI5 spanning the promoter to the body of the *U2af1-rs1* gene (Fig. 4A). This is consistent with our result that three genes, *Rik*, *Cct4*, and *B3gnt1*, are not imprinted. The unmethylated status of CGI4 is also consistent with the transcriptional interference model, in which *Murr1* imprinting results from the paternal transcription of *U2af1-rs1* and is not controlled by any *cis*-acting imprinting control elements. CGI5 showed both methylated and unmethylated statuses (Fig. 4A). This CGI has been reported as a DMR with a maternal allele-specific methylation (Hatada et al., 1995; Shibata et al., 1996; Feil et al., 1997). The result from our bisulfite sequencing of CGI5 agrees with the previous reports (data not shown). The fact that CGI5 is the only DMR in this region strongly supports the idea that this CGI is the ICR for the imprinting of *U2af1-rs1*.

In the human syntenic region of 399 kb, spanning from 83.8 kb upstream to 84.4 kb downstream of *MURR1*, 10 CGIs were identified and designated as CGI1 to CGI10. CGI1 is located downstream of the *FLJ* gene. CGIs 5, 6, and 7 reside in the introns of *MURR1*. Other CGIs are in the 5′ regions of the genes (Fig. 1B). Hot-stop COBRA analysis of the genomic DNA from human adult brain revealed that CGIs 2, 3, 4, 8, 9, and 10 were unmethylated and that CGIs 1, 5, 6, and 7 were methylated biallelically (Fig. 4B). None of the CGIs located at the 5′ region of the genes are methylated. Importantly, we could not find any differentially methylated CGI in this region. This result is also consistent with the conclusion that all the analyzed genes, including *MURR1*, are not imprinted in the tissues. The methylated CGIs are located in the introns of *MURR1* or downstream of *FLJ* gene. Biallelically methylated CGIs were identified in many human chromosomal regions, and some were closely linked to genes (Strichman-Almashanu et al., 2002). Biological functions of such methylated CGIs are not yet known.

3.5. 5′-Portion of the CpG island in U2af1-rs1 shows oocyte-specific methylation and is the putative ICR

Many imprinted genes are linked to DMR(s) in somatic cells. Among such DMRs, some are methylated in gametes, and the methylation is inherited by somatic cells. But others are unmethylated in gametes, and their methylation is established

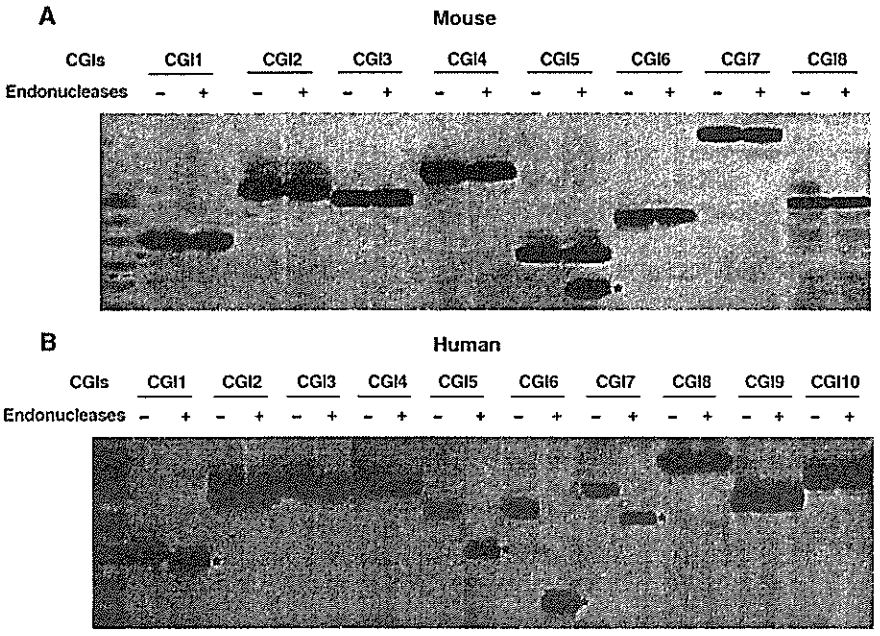

Fig. 4. Methylation statuses of CpG islands in mouse *Murr1* and human *MURR1* regions. Genomic DNAs from adult brains of human and BPF_1 mouse were subjected to methylation analysis by hot-stop COBRA. In this procedure, PCR amplification was performed on genomic DNA treated with sodium bisulfite. The PCR product of each CGI was electrophoresed after digestion with (+) or without (−) a restriction endonuclease. The cleaved PCR product, indicating methylation of the CGI, is marked with an asterisk. The PCR product can be cut with the restriction endonuclease only when the genomic DNA is methylated in the recognition site of the enzyme. Only CGI5 of mouse showed both the methylated and unmethylated bands, indicating a DMR, and all the others were unmethylated or methylated biallelically.

only during embryogenesis (Yatsuki et al., 2002). It has been considered that the primary imprint is the allele-specific methylation of DMR established in gametes and that the imprint also plays a central role in epigenetic regulation of the allele-specific expression of imprinted genes (Constancia et al., 1998; Ferguson-Smith and Surani, 2001). Shibata et al. (1997) reported that an oocyte-specific methylated region, termed region II, resided within the 5′ part of the large CGI5 of *U2af1-rs1*. They suggested that it was a strong candidate for the imprinting control element for *U2af1-rs1*. However, region II was in fact shown to be dispensable for the imprinted methylation of *U2af1-rs1* gene by Sunahara et al. (2000) using mice carrying targeted deletion of the *U2af1-rs1* CGI. In these mice, three fourths of the CGI, including region II, is deleted. The mice retained only the extreme 5′-portion of the CGI, corresponding to region I (Fig. 5D and Sunahara et al., 2000).

Based on these results, we assumed that the remained 5′-portion of *U2af1-rs1* CGI might be the imprinting control region of *U2af1-rs1* and therefore focused on this area for further analysis of gametic methylation. Sodium bisulfite sequencing was performed on genomic DNA of somatic tissues and male and female germ cells from BPF_1 or PBF_1 mice. We analyzed the 5′ half of *U2af1-rs1* CGI, spanning from the promoter to the large 5′ untranslated region of the gene, by dividing it into several regions (two are shown in Fig. 5A). In adult kidney, the maternal allele was completely methylated, and the paternal allele was unmethylated in all the regions analyzed, consistent with the previous reports (Hatada et al., 1995; Shibata et al., 1996; Feil et al., 1997). In the BPF_1 sperm, both parental alleles were completely unmethylated in all the regions analyzed. In the BPF_1 oocytes, the paternal allele was completely methylated in all regions. However, on the maternal allele, only the region designated as region a showed complete methylation and other regions, including region b, were not methylated. This methylation pattern of regions a and b was confirmed with the oocyte of PBF_1 mouse (Fig. 5B,C).

In the previous report by Shibata et al. (1997), region a was, however, composed of two parts with different methylation statuses. They showed, inconsistent with our results, that the 5′ part, designated region I, was unmethylated and the 3′ part, designated region IV, was methylated, both in oocyte and sperm (Fig. 5D). The region II was the oocyte-specific methylated region. But according to our analyses, region b, corresponding to region II, is not completely methylated in oocyte. Region a is the only DMR whose methylation is established in oocyte. Based on our results, we propose that the methylation is established as the primary imprint in region a in the early developmental stage of female germ cell and that this region is the ICR for the imprinting of *U2af1-rs1* gene. Region b was found to be methylated on the paternal allele but not on the maternal allele in oocyte (Fig. 5C). This differential methylation in region b indicates the following possibilities. The methylation established in region a may spread to adjacent regions, including region b. Region a may be methylated simultaneously on both alleles but the methylation spreads faster on the paternal allele than on the maternal allele. Alternatively, methylation may be established in region a on the paternal allele earlier than

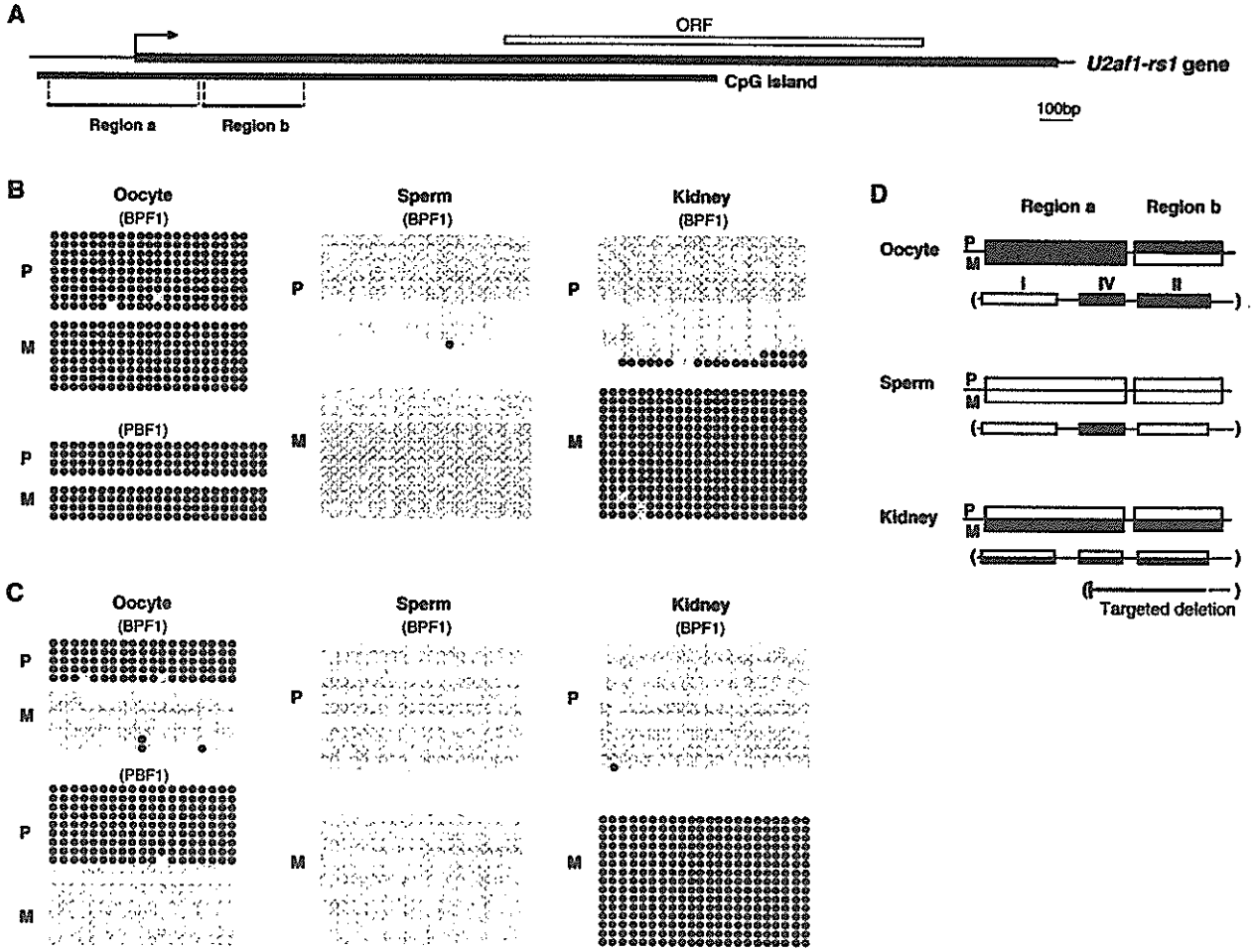

Fig. 5. Gametic methylation of the 5′-portion of *U2af1-rs1* CpG island. (A) Structure of *U2af1-rs1* gene. The intronless *U2af1-rs1* gene is shown as a solid box. Its open reading frame (ORF) and the CpG island are shown above and below the gene, respectively. The analyzed regions, a and b, within the CpG island are indicated by solid bars under the CpG island. (B) Gametic methylation of region a. Oocyte, sperm, and adult kidney were isolated from BPF_1 mice, and the DNAs were subjected to bisulfite-sequencing analyses. Oocyte from PBF_1 was also analyzed. Each row of circles represents the result of an independent PCR reaction. Each circle represents a CpG dinucleotide on the strand. A filled circle represents a methylated cytosine, and an open circle corresponds to an unmethylated one. P and M indicate the paternally inherited and the maternally inherited alleles, respectively. Kidney was used as representative of adult somatic tissues. (C) Gametic methylation of region b. (D) Schematic representation of methylation statuses of regions a and b in oocyte, sperm, and kidney. Open box, unmethylated; closed box, methylated. Region a in the CpG island showed oocyte-specific gametic methylation. Shown in parentheses are the previous reports on methylation of these regions by Shibata et al. The region of targeted deletion reported by Sunahara et al. is also shown.

on the maternal allele and then starts to spread earlier on the paternal allele. Both possibilities can result in the observed differential methylation of region b in the mature oocyte. Davis et al. (2000) reported that the methylation imprint in mouse *H19* DMR was established differentially on the parental alleles during male gametogenesis. *H19* DMR is methylated only on the paternal allele in somatic tissues. In primordial male germ cells at 13.5 day post coitum, the region is unmethylated on both alleles, indicating the erasure of the imprint. The methylation imprint was found to be re-established on the paternal allele earlier than on the maternal allele in the later stage of male germ cell development. These facts may indicate that parental alleles can be distinguished during male and female germ cell development and that re-establishment of imprint-methylation occurs on the paternal allele earlier than the maternal allele in both types of germ cell.

One possible reason for the discrepancy between our and Shibata's results is the different procedures employed for methylation analysis. Shibata et al. used methylation-sensitive PCR assay. This method depends on complete digestion of unmethylated genomic DNA with a methylation-sensitive restriction endonuclease, preceding PCR amplification, and can analyze only a few CpG sites in a region. In contrast to this procedure, the bisulfite sequencing method we employed is a more detailed and reliable method because all the CpG sites can be analyzed for their methylation statuses. The report by Sunahara et al., in which region b (region II) is dispensable for the *U2af1-rs1* imprinting, is consistent with our proposal that region a is the imprint mark and the ICR for *U2af1-rs1* gene. To elucidate the function of region a, more detailed functional analyses are needed, using transgenic and gene-targeted mice.

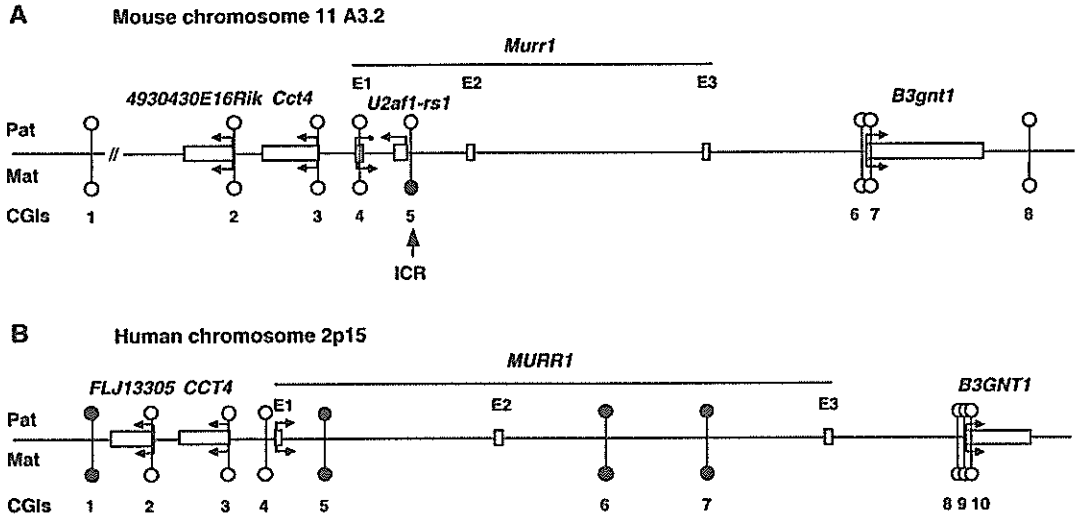

Fig. 6. Summary of allelic expressions of genes and methylation statuses of CpG islands in mouse *Murr1* locus (A) and human *MURR1* locus (B). Open boxes represent surrounding genes and exons of *Murr1* and *MURR1* genes. CGIs are shown by lollipops (closed for methylated CGIs and open for unmethylated CGIs). Horizontal arrows indicate allelic expressions and the directions of transcriptions. The results of paternal and maternal alleles are presented above (Pat) and below (Mat) the schematic maps, respectively. Note that the expression of mouse *Murr1* is repressed on paternal allele, irrespective of no differential methylation of the relevant CpG island. Position of the putative ICR is shown under the mouse map.

3.6. Conclusions

Human *MURR1* gene is an orthologue of mouse *Murr1* gene, which is imprinted in adult brain. The human gene is, however, not imprinted in adult and fetal brains. Mouse *Murr1* contains another imprinted gene, *U2af1-rs1*, in its 1st intron. It was suggested that the imprinted expression of *Murr1* was caused by the resident gene, *U2af1-rs1*. Consistent with the notion, non-imprinted human *MURR1* gene does not contain an orthologue of *U2af1-rs1* gene. Three surrounding genes of *MURR1* also showed biallelic expression in brain and other tissues and no DMR was found in this chromosomal region. These findings indicate that human *MURR1* locus is a non-imprinted locus. Mouse genes surrounding *Murr1* are in the same situation, that is, they are not imprinted and not linked to any DMRs. *Murr1* and *U2af1-rs1* are the only imprinted genes in this locus (Fig. 6). These facts led us to conclude that we have identified newly evolved imprinted locus in mouse genome after divergence of human and mouse.

In order to elucidate the imprinting mechanisms of mouse *Murr1* locus, *U2af1-rs1* is the most important gene to be investigated. For many imprinted genes their ICR have been shown to reside in the linked DMR, whose methylation is established in gamete and inherited to somatic cells during embriogenesis. *U2af1-rs1* gene has a large DMR which is methylated only on maternal allele in somatic cells. Within the DMR we have identified a region which is completely methylated in oocyte and unmethylated in sperm. This region is the most possible candidate for ICR of the gene and possibly of the locus.

Acknowledgments

We thank "Brain and Tissue Bank for Developmental Disorders, Baltimore, USA" for human adult brains and "Fetal Tissue Bank at University of Washington, Seattle, USA" for human fetal tissues. This work was supported by Grant No. 15570008 from the Ministry of Education, Culture, Sports, Science and Technology of Japan.

References

Constancia, M., Pickard, B., Kelsey, G., Reik, W., 1998. Imprinting mechanisms. Genome Res. 8, 881–900.

Cowles, C.R., Hirschhorn, J.N., Altshuler, D., Lannder, E.S., 2002. Detection of regulatory variation in mouse genes. Nat. Genet. 32, 432–437.

Davis, T.L., Yang, G.J., McCarrey, J.R., Bartolomei, M.S., 2000. The *H19* methylation imprint is erased and re-established differentially on the parental alleles during male germ cell development. Hum. Mol. Genet. 9, 2885–2894.

Feil, R., Boyano, M.D., Allen, N.D., Kelsey, G., 1997. Parental chromosome-specific chromatin conformation in the imprinted *U2af1-rs1* gene in the mouse. J. Biol. Chem. 272, 20893–20900.

Ferguson-Smith, A.C., Surani, M.A., 2001. Imprinting and the epigenetic asymmetry between parental genomes. Science 293, 1086–1089.

Fitzpatrick, G.V., Soloway, P.D., Higgins, M.J., 2002. Regional loss of imprinting and growth deficiency in mice with a targeted deletion of *KvDMR1*. Nat. Genet. 32, 426–431.

Hatada, I., Sugama, T., Mukai, T., 1993. A new imprinted gene cloned by a methylation-sensitive genome scanning method. Nucleic Acids Res. 21, 5577–5582.

Hatada, I., et al., 1995. Allele-specific methylation and expression of an imprinted *U2af1-rs1* (*SP2*) gene. Nucleic Acids Res. 23, 36–41.

Kitagawa, K., et al., 1995. Isolation and mapping of human homologues of an imprinted mouse gene *U2af1-rs1*. Genomics 30, 257–263.

Knight, J.C., 2004. Allele-specific gene expression uncovered. Trends Genet. 20, 113–116.

Kozak, M., 1987. An analysis of 5′-noncoding sequences from 699 vertebrate messenger RNAs. Nucleic Acids Res. 15, 8125–8148.

Lo, H.S., et al., 2003. Allelic variation in gene expression is common in the human genome. Genome Res. 13, 1855–1862.

Nabetani, A., Hatada, I., Morisaki, H., Oshimura, M., Mukai, T., 1997. Mouse *U2af1-rs1* is a neomorphic imprinted gene. Mol. Cell. Biol. 17, 789–798.